uOttawa

L'Université canadienne
Canada's university

FACULTÉ DES ÉTUDES SUPÉRIEURES ET POSTOCTORALES

uOttawa

L'Université canadienne
Canada's university

FACULTY OF GRADUATE AND POSDOCTORAL STUDIES

Arjun Shankar Rao

AUTEUR DE LA THÈSE / AUTHOR OF THESIS

M.A.Sc. (Chemical Engineering)

GRADE / DEGREE

Department of Chemical Engineering

FACULTÉ, ÉCOLE, DÉPARTEMENT / FACULTY, SCHOOL, DEPARTMENT

Carbonation of Fluidized Bed Combustion Solids

TITRE DE LA THÈSE / TITLE OF THESIS

Dr. E.J. Anthony

DIRECTEUR (DIRECTRICE) DE LA THÈSE / THESIS SUPERVISOR

Dr. Arturo Macchi

CO-DIRECTEUR (CO-DIRECTRICE) DE LA THÈSE / THESIS CO-SUPERVISOR

EXAMINATEURS (EXAMINATRICES) DE LA THÈSE / THESIS EXAMINERS

Dr. Christopher Lan

Dr. Handan Tezel

Gary W. Slater

Le Doyen de la Faculté des études supérieures et postdoctorales / Dean of the Faculty of Graduate and Postdoctoral Studies

Carbonation of Fluidized Bed Combustion Solids

By

Arjun Shankar Rao

Thesis submitted to the
Faculty of Graduate and Postdoctoral Studies
In partial fulfillment of the requirements
For the Master of Applied Science in Chemical Engineering

Department of Chemical Engineering
University of Ottawa

Your file Votre référence
ISBN: 978-0-494-25825-5
Our file Notre référence
ISBN: 978-0-494-25825-5

Abstract

Fluidized bed combustion (FBC) ash from the combustion of high-sulphur fuels with limestone addition can contain from 15 to 25% quick lime content. This excess calcium oxide gives the ash numerous undesirable properties such as strong exothermicity on wetting and high-pH leachate that must be treated before discharge. It also leads to the formation of ettringite with significant deleterious expansion in the landfill. In consequence, carbonation of FBC ash is desirable in order to reduce its alkalinity and improve its disposal characteristics.

The current technique to reduce the exothermic character of the ash involves hydrating the ash in two stages, leading to the consumption of large quantities of water. Sonication along with simultaneous carbonation of the ash yields a product suitable for direct disposal in landfills with the minimum of water addition (to achieve the optimum proctor levels for maximum compaction of the ash in the landfill site). This work explores the use of sonochemical-enhanced carbonation of FBC ash. Tests have been conducted using four ashes, two of which differ in age only and are from the Nova Scotia Power 183 MWe CFBC (circulating fluidized bed combustor) boiler. The other two ashes are from the CFBC boilers at A/C power and Piney Creek, U.S.A. Tests with additives such as sodium chloride (at levels comparable with that in seawater) and seawater from Nova Scotia have also been carried out. Tests were carried out at low (20°, 40°C) and high (60°, 80°C) temperatures. Sonicated samples were also analyzed using TGA (Thermogravimetric analysis), TGA-FTIR (Thermogravimetric and Fourier transform infra red spectroscopy analysis) and XRD (X-ray diffraction) techniques to determine the influence of other calcium compounds (OCC). The size reduction brought about by sonication was quantified using wet sieving.

The ash reactivity displays a strong temperature dependency with almost complete carbonation of the ashes being achieved in minutes at higher temperatures. Additives were found to increase the level of hydration of the ashes in line with previous work; however, carbonation levels were unaffected. TGA, TGA-FTIR and XRD analysis of the samples indicated that other calcium compounds (OCC) were also formed during hydration.

Sommaire

La cendre provenant d'un lit fluidisé pour la combustion (FBC) de carburants à haute teneur en souffre avec addition de pierre à chaux ($CaCO_3$) peut contenir 15 à 25% de chaux libre (CaO). L'excès de CaO donne à la cendre de nombreuses propriétés indésirables telles que qu'une forte exothermicité lors du contact avec l'eau et un lixiviat ayant un pH élevé qui doit être traité. Il mène également à la formation de l'ettringite avec une expansion néfaste dans le site d'enfouissement. En conséquence, la carbonation de la cendre de FBC est souhaitable afin de réduire son alcalinité et améliorer ses caractéristiques de disposition.

La technique courante pour réduire le caractère exothermique de la cendre requiert l'hydratation en deux étapes menant à une grande consommation d'eau. La sonification avec carbonation simultanée de la cendre donne un produit approprié à la disposition directe en site d'enfouissement avec un minimum d'addition d'eau. Ce travail explore donc l'utilisation de la carbonation sono-chimique de la cendre de FBC. Des essais ont été effectués avec quatre cendres dont deux diffèrent en âge seulement et proviennent du FBC de 183 MWe de Nova Scotia Power. Les deux autres cendres proviennent du FBC de A/C Power et Piney Creek, USA. Des essais avec des additifs tels que le NaCl (à une concentration comparable à celle de l'eau de mer) et l'eau de mer de la Nouvelle-Écosse ont été également effectués. Les tests ont été effectués à basses (20°, 40°C) et hautes (60°, 80°C) températures. Les échantillons sonifiés ont été analysés en utilisant des techniques de TGA, de TGA-FTIR et de XRD pour déterminer l'influence d'autres composés de calcium (OCC). La réduction de la taille des particules de cendres provoquée par la sonification a été mesurée en utilisant le tamisage humide.

La réactivité de la cendre dépend fortement de la température avec une carbonation presque complète en quelques minutes à températures élevées. Les additifs ont augmenté le niveau d'hydratation des cendres en accord avec des travaux antérieurs; cependant les niveaux de carbonation restent inchangés. L'analyse de TGA, de TGA-FTIR et de XRD des échantillons a indiqué que les OCC ont été également formés lors de l'hydratation.

Table of Contents

List of Tables

List of Figures

Acknowledgements

I would like to thank Dr. E.J. Anthony for the privilege of working on this project and for funding me throughout my Master's. I would also like to thank my co-supervisor Dr. Arturo Macchi for all the help that he has given me.

I am grateful to Dr. Lufei Jia, Dr. Yinghai Wu, Dr. Vasilije Manovic, Dr. Jean-Pierre Charland, Dr. Louis Giroux and Robert Dureau of CETC-O for their help. I would also like to thank the Department of Chemical Engineering, University of Ottawa. Finally, I would like to thank my family for their support and encouragement throughout my Master's.

1. Introduction

Coal is an important fuel source for power generation. Production of electric power from coal in an efficient and environmentally clean way is one of the greatest challenges facing the power industry. Fluidized bed combustion (FBC) technology produces clean power efficiently by utilizing coals of different grades with low emissions. Most coals available in North America have moderate to high sulphur content and require expensive add-on gas cleaning equipment to reduce SO_x emissions when utilized in conventional pulverized fuel (PF) fired boilers [1]. FBCs offer *in situ* capture of SO_x by the addition of limestone and are capable of burning coals containing moderate to high levels of sulphur. Alternate fuels like petroleum coke with low volatile content, high sulphur, very low ash and high heating values (~25-30 MJ/kg) are also being used for FBC power generation applications.

Several fluidized bed combustion technologies are currently available or are under development [2]. The two basic types are the bubbling fluidized bed combustor (BFBC) and circulating fluidized bed combustor (CFBC). Fluidized bed combustors typically have a round, square or rectangular cross-sectional configuration. A distributor is located at the bottom of the furnace and ensures uniform distribution of primary air through the combustor. The space above the bed is at least several metres tall and is known as the freeboard. The combustor contains a bed of solid particles which when slumped may typically be up to a metre deep. When sulphur capture is required, limestone particles are fed into the combustor. The limestone calcines and then reacts with the SO_2 evolved during combustion to form $CaSO_4$. The limestone particles do not sulphate completely and the bed consists of partially sulphated limestone particles along with coal ash-derived impurities and any tramp material in the coal feed. When sulphur capture is not required, sand or other refractory inert mineral particles are used in order to maintain the bed. When no air is flowing, the particle bed is 'slumped', *i.e.*, at rest on the bottom [2]. When air is introduced the bed remains static while the pressure drop across it increases with increasing flow rate. When the pressure drop becomes equal to the weight of the bed per unit area, the bed becomes suspended and increases in gas flowrate do not significantly affect the pressure drop and the bed is said to be fluidized. The superficial gas velocity at which the bed becomes suspended is called the minimum fluidizing velocity.

When the gas flow rate exceeds the minimum fluidization velocity the excess gas passes through the bed in the form of bubbles or slugs and causes the particles of the bed to undergo thorough mixing. The agitation also causes the movement of particles upward while the larger particles drop back and the finer particles are swept out of the combustor. The freeboard provides sufficient room for particles with terminal settling velocities lower than the superficial gas velocity to fall back into the bed. A cyclone separator is usually used to capture the bulk of the elutriated particles. If large numbers of particles are swept out of the bed, a part of the solid stream may be recycled, which both helps maintain the bed and enhances combustion efficiency. This type of combustor is known as a bubbling fluidized bed combustor; a diagram is presented in Figure 1.1.

With increasing gas flow rates, the elutriation of particles increases and at the same time the bubbling action changes to a more turbulent motion causing a strongly agitated and highly dispersed particle bed. At this point the distinction between the bed and the freeboard disappears and a significant particle charge can be maintained only by intense recirculation of the cyclone catch. This usually requires a large cyclone, which is operated hot and is lined with a refractory in order to help maintain the bed temperature **[2]**. This mode of operation in FBC is known as circulating fluidized bed combustion or CFBC; a diagram is presented in Figure 1.2.

FBC combustors are operated at bed temperatures in the range 800-900°C. The temperature limits are imposed at the lower end by the need for adequate combustion efficiency, and at the higher end of the range by ash softening problems and, when adding limestone, ensuring that there is optimum performance of the limestone for sulphur capture. Lower temperatures also ensure low NO_x emissions and most of the NO_x emitted from a FBC comes from the fuel nitrogen. During steady state operation, fuel and limestone are fed continuously and ash is continuously withdrawn from the bed itself or the hot cyclone, *i.e.*, bed ash, and after the final particulate removal stage, which is normally an electrostatic precipitator or a baghouse; this catch is known as fly ash. The various fluidization regimes with increasing gas velocity are presented in Figure 1.3.

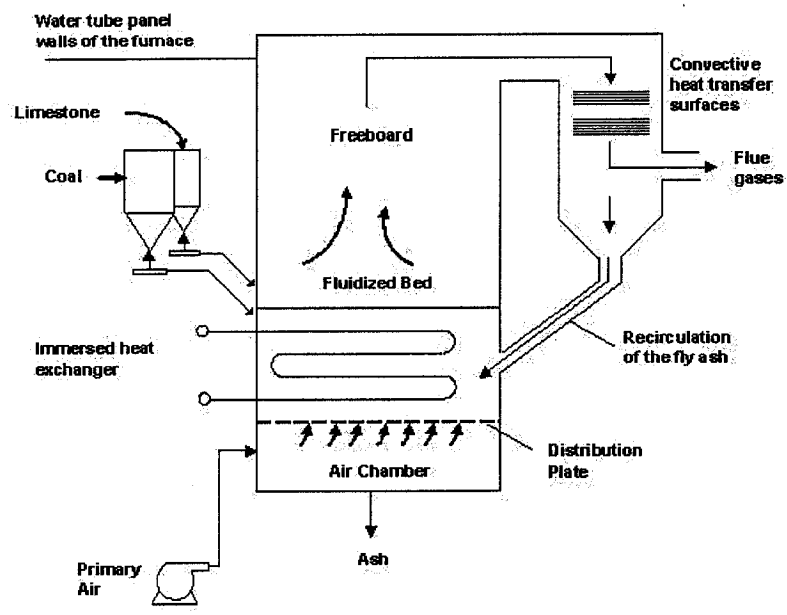

Figure 1.1: Bubbling fluidized bed combustor [3]

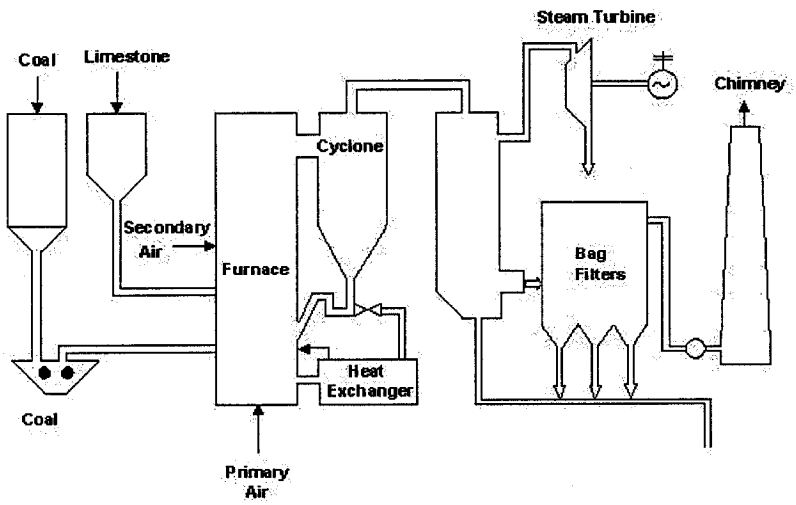

Figure 1.2: Circulating fluidized bed combustor [3]

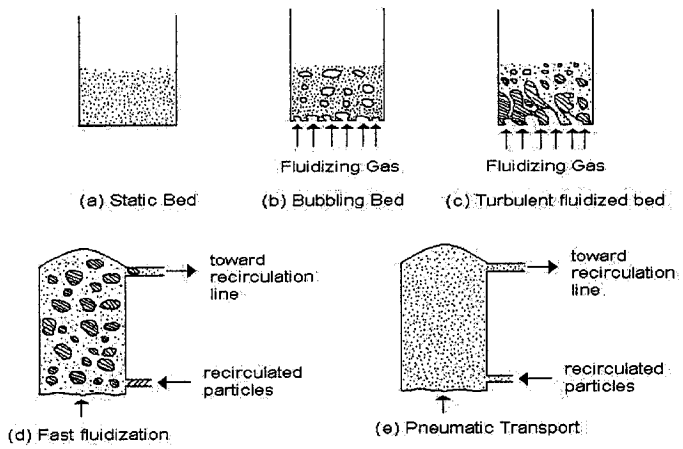

Figure 1.3: Fluidization regimes [3]

1.1. Classification of Fluidized Bed Combustors

Fluidized bed combustors can be classified into: atmospheric fluidized bed combustors (AFBC) and pressurized fluidized bed combustors (PFBC).

1.1.1. Atmospheric Fluidized Bed Combustors

AFBC technology has been in commercial use worldwide for well over 50 years, primarily in the petrochemical industry and in small industrial steam generators **[4]**. The features of in-bed capture of SO_2 and relatively low NO_x emissions along with the fluid bed's capacity to combust a range of different fuels are the main attractions of FBC as a power generation technology. In order to further commercialize this technology, manufacturers need to refine the technology to achieve lower capital costs than modern pulverized coal (PC) plants, improve operating efficiency *via* the development of supercritical steam cycles and improve environmental performance. The availability and cost of natural gas, along with competition from modern PC plants, determined the degree to which AFBC will compete with conventional technologies for power production. Since most new coal plants are currently being constructed outside North America, the greatest opportunity for this

technology lies in developing countries and there is evidence of major developments in this technology in China for example.

1.1.2. Pressurized Fluidized Bed Combustor

When a coal-fired fluidized bed combustor is operated at elevated pressure, the combustion gases themselves can be used for power generation by undergoing expansion in a gas turbine. However, the combustion products need to be sufficiently clean in order to prevent erosion, corrosion or fouling of the turbine **[5]**. Pressurized fluidized bed combustors (PFBC) produce lower levels of emissions and are smaller in size when compared to an equivalent atmospheric combustor. Due to the above benefits, this technology has been the subject of much research. Unfortunately the technology has not been able to resolve both cost and reliability issues and the vast majority of FBC boilers are of an atmospheric design.

1.2 Ash Disposal Problems

The sulphating reaction taking place in a FBC is inefficient and can result in the formation of an ash containing high levels of unreacted calcium oxide (up to 30%). Disposal of the ash in landfills gives rise to several problems. Compaction of the ash prior to landfilling requires that the ash be hydrated. The hydration reaction is highly exothermic and consumes large quantities of water. Dust generation is another hazard encountered during ash disposal. The free lime in the ash results in the formation of a high-pH leachate. The ash also contains silica and alumina along with several other components. Over extended periods of time (hours to days) aluminum and calcium compounds react to form compounds like ettringite ($3CaO.Al_2O_3.3CaSO_4.32H_2O$) which causes swelling of the ash and can eventually lead to the formation of cracks in the landfill lining.

In order to alleviate the above problems, processes like CERCHAR (research and development center of Charbonnage de France, French national coal company) and Ash Water Dense Suspension (AWDS) have been proposed. However, the above processes are unable to completely eliminate the production of high-pH leachate and also have problems with freeze-thaw cycles. Conversion of the unreacted calcium oxide to calcium carbonate

could solve most of the problems encountered when landfilling the ash. The carbonated ash could be used to generate carbon credits by utilizing the flue gas from the combustor as a source of carbon dioxide. Alternatively the carbonated ash could be reused as a sorbent for SO_2 capture in a FBC. This approach was investigated by CANMET Energy Technology Centre in Ottawa (CETC-O) and a process for carbonation of the FBC ash using sonic energy was proposed.

1.3 Thesis Objectives and Outline

The following points present the main objectives of this work:

1) Investigation of the effects of time and temperature on the carbonation of FBC ash using ultrasonics. Conversions are obtained using oven tests as well as thermogravimetric analysis.
2) Investigation of the effect of additives, both sodium chloride and seawater from Nova Scotia, on the carbonation of FBC ash.
3) Development of a rate expression for the carbonation reaction and calculation of activation energies.
4) Quantifying the effects of ultrasonics on the reaction by wet sieving and by comparison with stirring.

The thesis outline is as follows: A brief description of the various processes that have been proposed, a brief literature survey of the carbonation reaction and background on ultrasonics are presented in Chapter 2. Chapter 3 provides a description of the experimental setup as well as the measurement techniques used. Chapter 4 presents the results and discussion. Conclusions as well as future recommendations are presented in Chapter 5.

2. Current Ash Disposal Strategy

Ash from CFBCs burning high-sulphur fuels differs from standard pulverized coal-fired (PC) ash due to the presence of limestone-derived products from the sulphur dioxide capture process. Residue from Nova Scotia Power, which is typical of ash from a CFBC unit burning high-sulphur fuel, contains calcium sulphate (~30-35%), calcium oxide (~15-25%), calcium carbonate (~3 to 4%), Fe_2O_3, SiO_2, Al_2O_3 and other coal ash compounds (~40-45%) **[6]**. Contact with water results in hydration, an exothermic chemical reaction which generally converts CaO to $Ca(OH)_2$ and, more slowly, $CaSO_4$ to hemihydrate and eventually gypsum ($CaSO_4.xH_2O$, where x = ½ or 2). Other reaction products include calcium sulphoaluminate compounds. Water addition to CFBC residue not only provides for control of dust handling and transfer operations, but also completes these hydration reactions as part of meeting disposal objectives **[6]**.

Large quantities of ash are produced during the combustion of coal in a FBC. For example it was estimated that 284000 tonnes of ash would be produced by the 183 MWe CFBC at Point Aconi, Nova Scotia, when combusting coal with high ash content over a period of one year. The ash produced in the FBC is stored in silos. The CFBC at Point Aconi utilizes two silos with capacities of 2218 and 554 tonnes to store fly ash and bed ash respectively **[7]**. The ash is discharged from the silos either in the wet or dry condition. Dry ash finds potential use in other applications like waste stabilization, nonstructural backfill, *etc.* Wet unloading of the ash is typically carried out in order to landfill the ash. The ash is unloaded from the silos using mixer/unloader units with simultaneous water addition. The rate of water addition is calculated based on dust control as well as water consumption during the exothermic hydration reaction. This water addition is known as primary water addition.

The hydrated ash is transported to the landfill site in dump trucks that are modified to provide dust control. Water trucks at the placement site provide sufficient water for hydration of the ash. The main objectives of compaction and placement of the ash are to maximize the compacted density of the conditioned ash and to minimize water contact with the residue once it has been placed in the landfill. The first objective is achieved by water addition at the landfill site while the second objective can be achieved by proper design of the landfill site. A summary of the residue management process is presented in Figure 2.1.

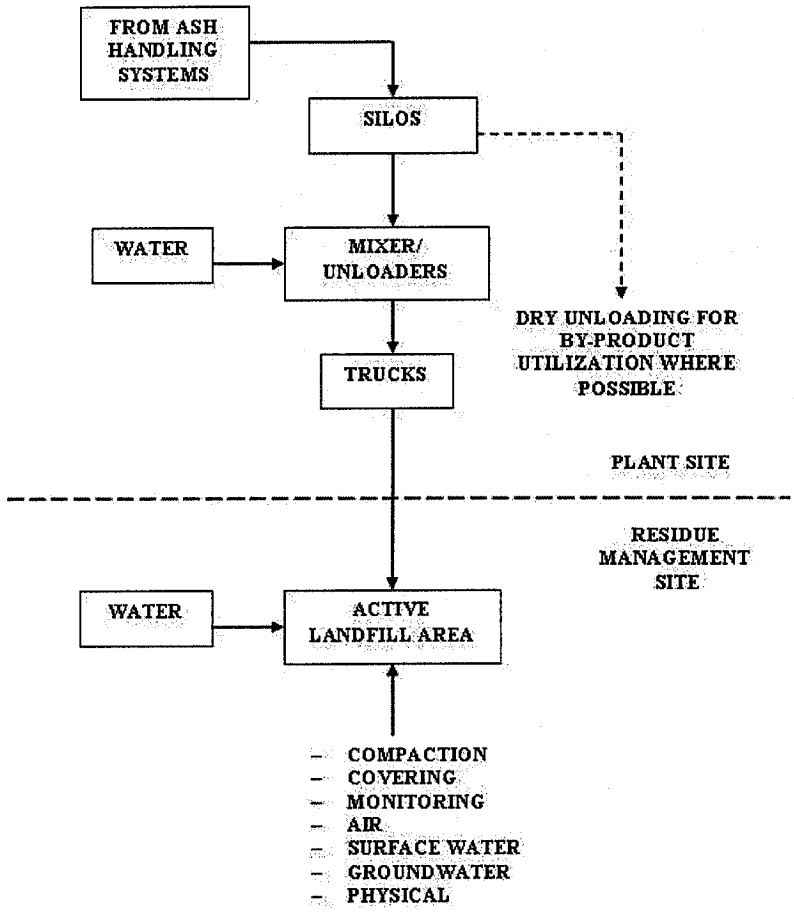

Figure 2.1: Residue management process [7]

2.1 Alternative Processes

Several processes have been proposed in order to find a solution to the ash disposal problem and are described below.

2.1.1 CERCHAR Process

CERCHAR is the R&D centre of the French national coal company **[8]**. In the late 1980s, CERCHAR started work on a slaking technique to treat ashes from a 600MWe pulverized coal-fired boiler burning a 3.8% sulphur brown coal from Gardanne, France. This

coal had a natural Ca/S molar ratio of 1.6-2.6 leading to a chemical residue quite similar to FBC ashes. In order to allow these ashes to be used for other applications like addition to Portland cement, CERCHAR determined that the free lime content must be less than 5%. Practical handling requirements also demanded a dry product (<0.5% moisture).

This led to the development of a technique, which involved hydration of the residue in a batch reactor capable of withstanding high pressures due to expansion of steam produced by slaking and was patented by CERCHAR in 1990. The hydration reaction was carried out at 130°C and prevented the formation of ettringite or similar compounds. It was CETC-O's belief that this technology could offer considerable advantages when utilizing CFBC ash, including the complete suppression of the exothermic behavior of CFBC ashes. It was also hoped that this process could control the destructive expansion seen with FBC ash disposal. In addition, it is well known that excessive free lime contents are also associated with destructive expansion in Portland cements **[8]**. However, tests using this method revealed that although the CERCHAR process was able to control the exothermic behavior of FBC ash, the ash still displayed poor freeze-thaw stability and the process still allowed the production of high-pH leachate. A diagram of the CERCHAR process is presented in Figure 2.2.

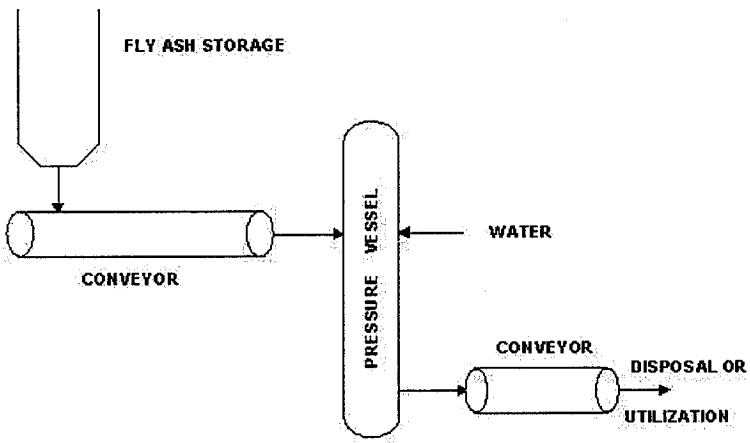

Figure 2.2: CERCHAR process [8]

2.1.2 Ash Water Dense Suspension (AWDS) Technology

The AWDS method for disposal of power station wastes was developed in Poland and has since been used in Poland and Hungary for ash disposal. Initial development of this technology utilized ashes from pulverized coal combustion. In this method ash and water are mixed together to form concentrated suspensions or emulsions. The solid-to-water ratios used vary from 1:1 to 3:1. These emulsions behave like thixotropic non-Newtonian fluids and allow the mixtures to be pumped to the disposal site **[9]**. The mixture then sets over a period of time to produce solids similar to soft rock without any water separation. These solids displayed high densities, low permeabilities and high unconfined compressive strengths showing that they could be used for applications such as linings for landfill sites. A diagram of the AWDS technology is presented in Figure 2.3.

The use of this technology for disposal of FBC boiler-derived ashes was investigated by CETC-O with support from Environment Canada, Nova Scotia Power Inc., Cracow University of Technology and the Polish government laboratory AGH in 1991. The ashes tested were from the 0.8 MW CFBC operated at CETC-O laboratories in Ottawa, Ontario using Devco Prince Coal and several high-calcic limestones from Nova Scotia. Initial studies indicated that the suspensions remained fluid long enough to permit hydraulic transport and did set like ashes from conventional pulverized coal combustion **[9]**. However, narrow ash-to-water ratios of 1.24 for bed ash and 1.5 for the combined solids were required. Strength development of up to several MPa was noted with these samples and permeabilities were also very low and were comparable to ashes from pulverized coal combustion. However, further research indicated that the solids produced by this method had significant problems with freeze-thaw behavior, limiting the usage of this technology.

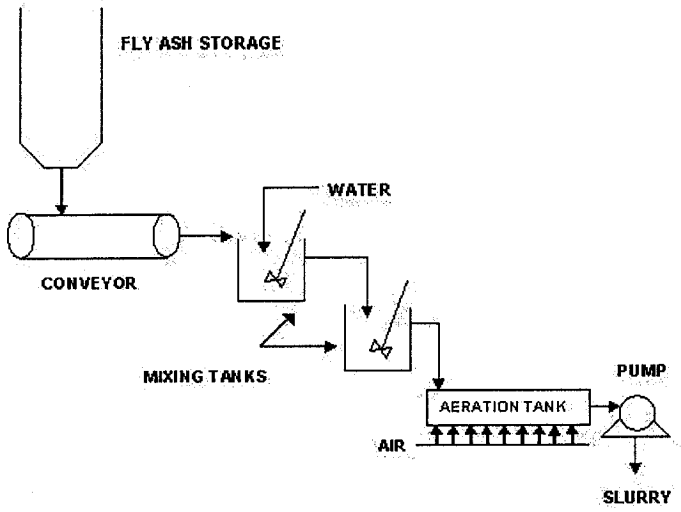

Figure 2.3: AWDS process [8]

2.1.3 CETC-O Reactivation Technique

Since both the CERCHAR and AWDS process did not meet all the requirements for the safe disposal of FBC residue, CETC-O and General Comminution Inc. developed a wet grinding technique to hydrate the ash. The product from this process was to be reused as a sorbent in the combustor. FBC ash typically consists of an unreacted calcium oxide core surrounded by a sulphate shell. This method proposed to hydrate the ashes by grinding the ash in a wet condition, which would allow for the breakage of the sulphate shell and grant access to the unreacted CaO core. The wet hydrated ash could then be pneumatically conveyed to the combustor. Subsequent bench-scale CFBC tests by CETC-O demonstrated the effectiveness of this approach.

The disadvantage of the above process was that the wet product quickly underwent self-cementing reactions, and in practice would be difficult if not impossible to feed reliably to an industrial-scale combustor. One of the solutions proposed was to mix the wet slurry with fresh fuel which would allow the spent sorbent to form pellets while the excess water was absorbed by the fresh fuel. This would prevent the formation of cement-like particles from the sorbent present in the slurry. Hydration of the ash particles would not be affected as the hydration reaction was expected to be nearly complete during grinding. In this manner it was

thought to achieve quantitative hydration of the CaO in the sorbent, and still deliver a dry product. However, while this technology has been demonstrated at the full scale **[10]**, it is yet to be commercialized.

2.2 Carbonation

Limestone ($CaCO_3$) is used in fluidized bed combustors for sulphur capture. This process suffers from low sorbent utilization **[11]**. The calcined limestone sulphates poorly, with a maximum conversion to calcium sulphate of 50-60% due to pore blockage caused by high molar volume calcium sulphate, which prevents further utilization of the sorbent. This spent sorbent can be reactivated to be reused for sulphur capture by ensuring exposure of the CaO from the interior of the sorbent particle **[11]**.

When hydrated, CaO reacts with water to form $Ca(OH)_2$ which in turn reacts with CO_2 to form $CaCO_3$ as shown in the following reactions.

$$CaO + H_2O \rightarrow Ca(OH)_2 \quad (2.1)$$

$$Ca(OH)_2 + CO_2 \rightarrow CaCO_3 + H_2O \quad (2.2)$$

FBC solids typically consist of an unreacted CaO core surrounded by a sulphate shell. In order to undergo carbonation the CO_2 would have to diffuse through the sulphate shell leading to a reduction of the reaction rate. Furthermore as the reaction proceeds the $CaCO_3$ formed would also limit the reaction rate due to pore blockage.

2.2.1 Ultrasonics

Ultrasound has proven to be a very useful tool in enhancing the reaction rates in a variety of reacting systems **[12]**. It has been successfully used to increase conversion, improve yield and initiate reactions in chemical, electrochemical and biological systems and is finding widespread use in the laboratory. Ultrasound is slowly gaining acceptance in the industry as it offsets or eliminates other process costs by enabling operations at lower temperatures and pressures, eliminating the use of expensive solvents, *etc.*

Ultrasound occurs at a frequency higher than the audible frequency of the human ear, and is usually associated with the frequency range of 20 kHz to 500 MHz. Low-intensity, high-frequency ultrasound (in the megahertz range) does not alter the state of the medium through which it travels and is commonly used for nondestructive evaluation and medical diagnosis **[12]**. However, high-intensity, low-frequency ultrasound alters the state of the medium and is typically used for sonochemical applications.

Ultrasonics requires a liquid medium to transfer energy efficiently. One of the main effects of ultrasound when used in conjunction with a liquid is cavitation. Cavities formed in a liquid are in the form of bubbles. Specks of dust or pockets of gas trapped in the liquid act as nuclei leading to bubble formation. When ultrasonic waves propagate through a liquid they create mechanical disturbances in the form of pressure fluctuations. A reduction in pressure below the liquid pressure causes the bubble to grow while an increase in pressure above the liquid pressure causes bubble collapse. Due to the rapidity of the collapse large instantaneous local pressures and temperatures are developed **[13]**. Two competing theories exist to explain the chemical effects due to cavitation: the hot-spot theory and the electrical theory **[12]**. According to the hot spot theory when bubbles undergo cavitation localized hot spots are formed which reach temperatures and pressures in excess of 4727°C and 50 MPa, see Figure 2.4. The electrical theory postulates that an electrical charge is formed on the surface of a cavitation bubble leading to the formation of enormous electrical field gradients across the bubble that are capable of breaking chemical bonds upon bubble collapse. The hot-spot theory is more generally accepted.

Numerous studies have been performed on bubble growth and collapse and the bubble size can be calculated by using the following equation:

$$R\check{R} + 3/2\ \check{R}^2 = 1/\rho\ [p_L(R)-p_\infty(t)] \qquad (2.3)$$

Where p_∞ is the pressure in the liquid far from the bubble, ρ is the density of the fluid, R and $\check{R}$ represent the first and second order time derivatives of the bubble radius and $p_L(R)$ is the liquid pressure just outside the bubble wall, given by the following equation:

$$p_L(R) = p_T(R) - 4\mu(\check{R}/R) - (2\sigma/R) \qquad (2.4)$$

Where μ is the viscosity of the bulk liquid medium and σ is the surface tension of the bulk liquid medium. Equations 2.3 and 2.4 are based on the assumption that the liquid is incompressible and the viscous forces are neglected. The pressure far from the bubble in an acoustic field with a pressure amplitude P_A and angular frequency ω is given by:

$$p_\infty(t) = P_o - P_A \sin(\omega t) \qquad (2.5)$$

Where P_o is the hydrostatic (ambient) pressure **[12].** Typical initial bubble sizes range between 5-10 μm for acoustic cavitation.

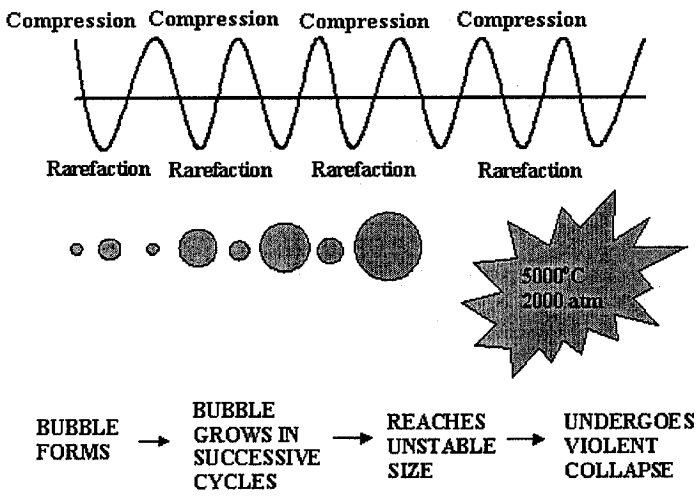

Figure 2.4: Development and collapse of cavitation bubbles [14]

The implosive collapse of microbubbles also results in a variety of mechanical effects. Here we believe it is the mechanical effects that are important for the carbonation process. In the case of a heterogeneous reaction, when solid particles are near the cavitation bubble, the implosion may occur symmetrically or asymmetrically, depending on the proximity of the solids. Symmetric cavitations create shock waves that propagate to the surrounding solids causing microscopic turbulence and/or thinning of the solid-liquid film **[15]**. This phenomenon is called microstreaming and is thought to be the cause for increases in the rate of mass transfer of reactants and/or products. When solid particles are near the bubble, it is unable to collapse symmetrically. This causes asymmetric cavitation and is responsible for the formation of microjets of solvent which impact on the solid surface, causing pitting and

erosion, see Figure 2.5. Ultrasound can increase the rates of reaction and mass transfer through these mechanical effects alone, even if it does not influence the reaction chemically [15]. As the carbonation of FBC ash is limited by transfer of CO_2 across the sulphate layer, it was suggested that ultrasonics could be used to alleviate this problem.

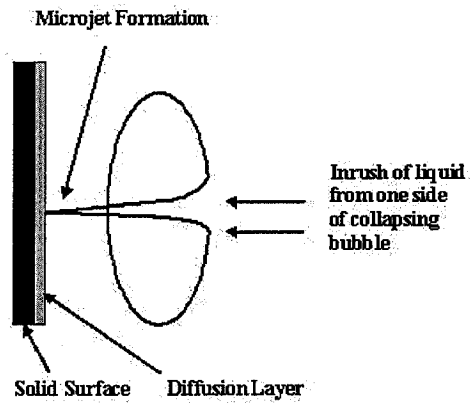

Figure 2.5: Cavitation bubble collapse near a solid surface [14]

2.3 Reaction Kinetics

Jia *et al.* [16] have shown that carbonation of the ash is very slow when carried out at temperatures below 400°C without prior hydration. At such temperatures it is believed that CaO hydrates to $Ca(OH)_2$ which in turn carbonates to $CaCO_3$. A number of studies on the carbonation of lime have been carried out in literature. Juvenkar and Sharma [17] have proposed the following equations for the carbonation of a suspension of lime:

$$Ca(OH)_2\ (s) \leftarrow\rightarrow Ca^{2+}\ (aq) + 2\ OH^-\ (aq) \qquad (2.6)$$

$$CO_2\ (g) \leftarrow\rightarrow CO_2\ (aq) \qquad (2.7)$$

$$CO_2\ (aq) + OH^-\ (aq) \rightarrow HCO_3^-\ (aq) \qquad (2.8)$$

$$HCO_3^-\ (aq) + OH^-\ (aq) \rightarrow H_2O + CO_3^{2-}\ (aq) \qquad (2.9)$$

$$Ca^{2+}(aq) + CO_3^{3-}(aq) \rightarrow CaCO_3(s) \quad (2.10)$$

They had also developed the rate expressions for the overall process. In the case of FBC ash, other calcium compounds (OCC) such as gehlenite ($2CaO.Al_2O_3.SiO_2$), larnite ($2CaO.SiO_2$), di-calcium ferrite ($2CaO.Fe_2O_3$), *etc.* can also be present and they may complicate the analysis because they affect the amount of free lime present in the system. It is common in FBC literature to assume that the only Ca compounds are CaO and $CaSO_4$, unless reaction with the atmosphere has taken place, in which case $Ca(OH)_2$ and $CaCO_3$ may also be present. Unfortunately, with real ashes this may not be the case and OCC complicate data analysis in hydration and carbonation experiments.

Due to the difficulty in characterizing the various reactions that can possibly occur, it is assumed that the following reaction is simply a global reaction:

$$CaO + CO_2 \rightarrow CaCO_3 \quad (2.11)$$

The above reaction can be assumed to be irreversible and first order with respect to CaO, *i.e.*, the rate is proportional to the concentration of CaO. The expression for the rate of a first order reaction is given by

$$\frac{-dC_A}{dt} = -r_a = kC_A \quad (2.12)$$

In terms of conversion, the above rate expression can be written as

$$\frac{dX_A}{dt} = k(1 - X_A) \quad (2.13)$$

Rearranging and integrating the above expression gives

$$-\ln(1 - X_A) = kt \quad (2.14)$$

A plot of $-\ln(1-X_A)$ *vs.* t for a first order reaction gives a straight line passing through the origin, with the slope giving the value of the rate constant k. The temperature dependency of the reaction rate appears to be well represented by the Arrhenius Law **[18, 19]**:

$$k = k_0 e^{-\frac{E}{RT}} \tag{2.15}$$

The values of the activation energy and the frequency factor can be obtained by plotting ln k *vs.* 1/T. The slope of this plot gives the value of -E/R **[18, 19]** from which the activation energy E can be determined.

3. Experimental Setup and Operating Procedure

The experimental setup is shown in Figure 3.1. The setup consists of a 200 ml double-walled glass sample holder that is connected to a water circulation unit with a digital temperature controller manufactured by Polyscience. The temperature can be maintained by using the temperature controller and the sample temperature is maintained at the desired level by water circulation. The sample pH is measured using a digital pH AP-63 meter manufactured by Fischer Scientific. Pure CO_2 is supplied to the system by means of a tube connected to a pressurized CO_2 cylinder. The flow rate of the gas is controlled by a rotameter manufactured by Matheson. The ultrasonic unit consists of an ultrasonic probe and a control unit. The probe and control unit are manufactured by Sonics and Materials. Two units, rated at 600W (VCX600) and 750W (VCX750), have been utilized. The experimental procedure is as follows for the batch tests.

The temperature controller along with the circulation unit is switched on and the desired temperature is selected. When the temperature controller reports a steady value, 10g of the bed ash is weighed and transferred to the sample holder. 100mL of deionized water (tap water for tests with ash from Piney Creek and A/C power, USA) is added to the sample holder and the pH of the mixture (100ml) is measured. The ultrasonic control unit is then switched on and parameters of time and amplitude are selected. In the case of the older VCX 600 unit, tuning of the control unit was carried out immediately on startup. The ultrasonic probe is then dipped in the solution and gas flow is started. The probe is then switched on and the pH of the sample is again measured upon completion of the run. The solids are then filtered off using a filter utilizing Whatman No.41 ashless filter paper connected to a vacuum pump. The sample is then dried in an oven for 1 h at 110°C, cooled in a desiccator and stored. The same procedure is used for tests in which the ultrasonic probe is replaced by the stirrer (BDC 2002) manufactured by Caframo. The stirrer speed is maintained at 700 rpm.

The semi-continuous sampling tests are carried out in the same manner as the batch tests using the VCX 750 unit. The temperature controller along with the circulation unit is switched on and the desired temperature is chosen. When the temperature controller reports a steady value, 10g of the bed ash is weighed and transferred to the sample holder. 100mL of

tap water is added to the sample holder. The ultrasonic control unit is then switched on and parameters of time and amplitude are set. The ultrasonic probe is then dipped in the solution and gas flow is started. The probe is then switched on and 5 ml of the reaction mixture is withdrawn at 5, 10, 15, 20 and 25 minutes using a syringe and simultaneously filtered by a filter utilizing a Whatman No.41 ashless filter paper connected to a vacuum pump. The samples are then dried in an oven for 1 h at 110°C, cooled in a desiccator and stored.

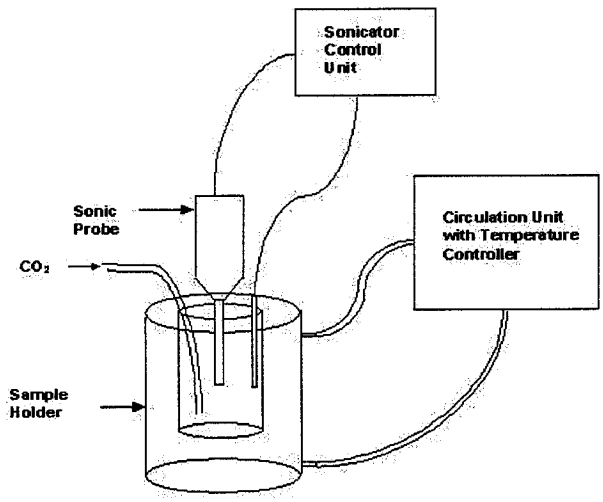

Figure 3.1: Experimental setup

3.1 Measurement Techniques

Several measurement techniques have been used to characterize the ash samples and are described below.

3.1.1 Oven Tests

The degree of hydration as well as carbonation can be determined by oven tests. It is well known in literature **[20]** that $Ca(OH)_2$ decomposes in a temperature range of 400-500°C and that at CO_2 partial pressures typical of atmospheric conditions, $CaCO_3$ decomposes in the temperature range of 600-800°C. Hence, the weight lost by evolution of water and CO_2 at the appropriate temperature ranges should be able to give a measure of the conversion of CaO to

$Ca(OH)_2$ and $CaCO_3$. One of the benefits of using an oven test is that it provides reasonable results in most cases and is easy to carry out for a large number of samples. Oven tests are carried out by heating around 0.5g of the sample in an oven to a temperature of 500°C for a time period of 1 h. The weight of the sample is noted before and after heating. The same sample is then heated to a temperature of 800°C for the same time period, and corresponding weights are noted.

$Ca(OH)_2$ and $CaCO_3$ are formed by reaction with H_2O and CO_2 respectively:

$$CaO + H_2O \rightarrow Ca(OH)_2 \tag{3.1}$$

$$CaO + CO_2 \rightarrow CaCO_3 \tag{3.2}$$

Based on the stoichiometry of the above reactions the conversion of CaO to $Ca(OH)_2$ as well as $CaCO_3$ can be calculated by using the following formulae

$$Ca(OH)_2 \text{ expressed as } \%\ CaO = \left(\frac{56}{18}\right) * \left(\frac{\text{Weight lost due to evolution of } H_2O}{\text{Total weight of the sample}}\right) * 100 \tag{3.3}$$

$$CaCO_3 \text{ expressed as } \%\ CaO = \left(\frac{56}{44}\right) * \left(\frac{\text{Weight lost due to evolution of } CO_2}{\text{Total weight of the sample}}\right) * 100 \tag{3.4}$$

The conversions are then calculated based on the original CaO content obtained from the free lime test using the following formula

$$X_A = 1 - \frac{C_A}{C_{Ao}} \tag{3.5}$$

3.1.2 Thermogravimetry (TGA) and Fourier Transform Infrared (FTIR) Analysis

TGA is a technique in which the mass of a substance is monitored as a function of temperature or time as the sample specimen is subjected to a controlled temperature program in a controlled atmosphere **[21]**. In order to carry out a thermogravimetric analysis the

instrument used needs to be capable of both simultaneous heating and weighing. Hence, the instrument used for performing thermogravimetric measurements is often referred to as a thermobalance. A thermobalance is usually made up of the following components: sensitive recording microbalance, furnace with integrated enclosure for heating the sample specimen, temperature programmer, heater with associated control circuitry and electronics, pneumatic system for dynamic purging of the furnace/sample chamber, data acquisition system and purge gas switching device. Purge gas switching capability is required only for those applications in which the purge gas is changed during the experiment. Modern TGA systems are usually computer controlled. Many commercial TGA systems are available and the major differences in these are in the furnaces (size, design, and positioning), degree of microcomputer control of the hardware, and in the capabilities of the data acquisition systems offered with the thermal analysis system **[21]**.

Thermal curves obtained from thermogravimetry give very accurate and precise measurements of weight; however, the measurement of temperature is not as accurate. Reasons for loss of accuracy in temperature measurement are usually due to the fact that the thermocouple is not in actual contact with the sample as it is normally placed very close to the sample pan. Also the composition and flow rate of the gases used for the experiment influence the sample temperature. The composition of the purge gas is based on the analysis being carried out. For example, in case of a pyrolysis reaction, either nitrogen or argon is commonly used. Evolved gas analysis (EGA) is used for the simulation of many industrial processes in which materials are heated, for establishing decomposition mechanisms, and for determining the stoichiometric relationships for such decompositions **[21]**. Several TGA-EGA systems are described in literature, analyzing the evolved gases by different techniques, *i.e.*, thermal conductivity, cold trapping followed by gas chromatography (GC), mass spectrometry (MS) and infrared (FTIR) **[22]**. FTIR is normally used to measure gas phase spectra and can also provide quantitative determinations.

The TGA used for analysis of the sonicated samples is a Perkin Elmer TGA-7 thermogravimetric analyzer. The tests are carried out in a nitrogen atmosphere with a heating rate of 10deg/min. The speciation of the gases evolved during the TGA test as well as the rate of evolution of the gases is determined using FTIR. A typical TGA curve for a sample sonicated at 40°C and 60 min is shown in Figure 3.2. From the figure two weight losses can

be seen which correspond to the loss of water and CO_2. Conversions of CaO to $Ca(OH)_2$ as well as $CaCO_3$ are calculated based on the same calculations used for the oven test.

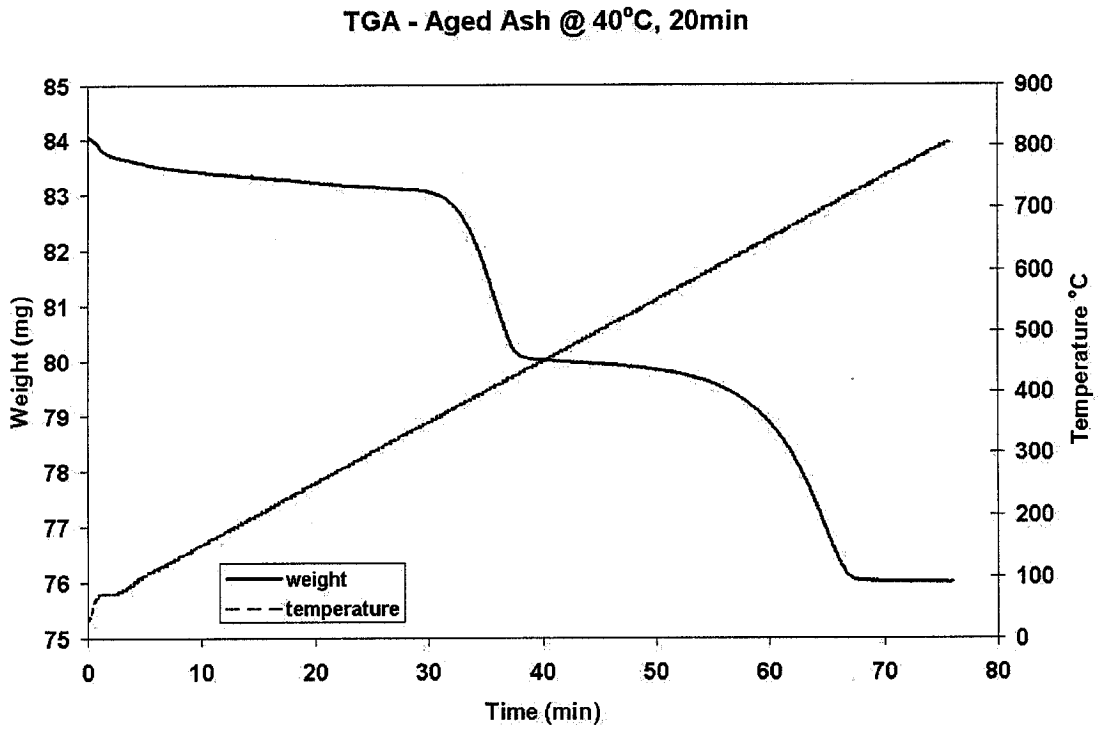

Figure 3.2: TGA curve for sample sonicated at 40°C, 60 min

3.1.3 ASTM (American Society for Testing and Materials) Modified Quick Lime Test

The modified quick lime analysis is carried out before sonication in order to determine the free CaO and $Ca(OH)_2$ contents of the bed ash. The following apparatus is required for the test: burette, conical flasks, 200 ml beaker, 2 two-liter beakers, 3 magnetic stirrers with heaters and 3 magnetic pellets. The chemicals required for the test are: 0.1 M hydrochloric acid, 0.1 M sodium hydroxide, phenolphthalein indicator – 4%, and sugar or sucrose.

The procedure for conducting the modified quick lime test is as follows. About 1 liter of CO_2-free water is heated in a beaker. The required amount of sugar (depending on the

number of trials being conducted) is weighed out. For example, if 4 trials are being conducted, 4*20g = 80 g of sugar is required. The sugar is dissolved in warm water (for example, 80g of sugar requires 160 ml of water) with constant stirring using a magnetic stirrer with pellet. After the sugar has dissolved completely in the water about 1-2 drops of phenolphthalein indicator is added followed by 2-3 drops of 0.1 M sodium hydroxide solution until the solution turns pale pink in color.

Approximately 0.2 g of the bed ash sample is weighed in a clean and dry conical flask. 50 ml of hot water is added to the flask and simultaneous heating and stirring of the flask using a magnetic stirrer and pellet are carried out until the water starts to boil. The water in the conical flask is boiled for 1 minute and then cooled to room temperature. 50 ml of sugar solution is added to the conical flask along with 2-3 drops of phenolphthalein indicator. The solution is stirred using a magnetic stirrer with pellet for 13 minutes. The solution is then titrated against 0.1 M HCl taken in a burette until the pink color disappears. The end point of the reaction is the first disappearance of the pink color as it reappears after a few moments.

The amount of CaO and $Ca(OH)_2$ present in the ash can be calculated using the following formula: %CaO + $Ca(OH)_2$ = 0.2804* Vol. of 0.1M HCl run down (ml)/weight of sample

3.1.4 Wet Sieving

A number of techniques are available to measure the size of a particle. Sieve analysis normally gives information about particles greater than 50 μm in size. Particle size analysis of the bed ash prior to sonication is carried out using dry sieving. However, when the bed ash is sonicated at temperatures of 60° and 80°C the ash particle undergoes size reduction and forms a slurry. Due to the cementatious nature of FBC bed ash the sonicated ash forms lumps on drying. Therefore, water is used during sieving to prevent agglomeration of the particles.

The procedure utilized for wet sieving is as follows. Mesh sizes of 1.4 mm, 1.0 mm, 850 μm, 600 μm, 425 μm, 250 μm, 125 μm, 75 μm and 38 μm are used. Dry sieving of the bed ash prior to sonication is carried out and the fines are collected in the pan. Sieving is carried out using 50g of bed ash for 20 min using a Haver-Tyler EML 200 digital7 test sieve shaker and the weight of each screen before and after sieving is noted down. The sample is then

thoroughly mixed and 10g of the bed ash is subjected to sonication at temperatures of 20, 40 and 60°C for 40 min. The sonicated sample is then discharged onto the stack of screens and sieved using water to prevent agglomeration of the sample. The screens are then dried in a furnace at 110°C for one hour, cooled and then weighed. The fines that pass through the screens are filtered using a Whatman no. 41 ashless filter paper (20-25 μm), dried at 110°C for one hour and then weighed. A particle size analysis is carried out using the following calculation (Table 3.1) and a cumulative weight-size distribution graph is plotted.

Table 3.1: Size distribution calculation

Particle Size, μm	Empty weight of sieve, g	Weight of sieve with sample, g	Weight of sample, g	Weight fraction	Weight %
1400	448.84	454.66	5.82	0.0000	-
1000	442.28	442.72	0.44	0.0047	0.47
850	464.08	464.44	0.36	0.0038	0.38
600	433.01	436.6	3.59	0.0381	3.81
425	376.48	386.18	9.7	0.1030	10.30
250	396.22	427.83	31.61	0.3356	33.56
125	359.7	401.82	42.12	0.4472	44.72
75	358.88	364.45	5.57	0.0591	5.91
38	328.1	328.71	0.61	0.0065	0.65
pan	372.77	372.95	0.18	0.0019	0.19
total			94.18	1	100

3.1.5 Statistics

Statistical analysis can be used to summarize a situation, model experimental outcomes, make decisions, quantify uncertainty, *etc.* **[23].** Some of the basic definitions used are:

a) Mean

$$\bar{y} = \frac{1}{n}\sum_{i=1}^{n} y_i \tag{3.6}$$

b) Sample Variance

$$s^2 = \frac{1}{n-1}\sum_{i=1}^{n} (y_i - \bar{y})^2 \tag{3.7}$$

c) Sample Standard Deviation

$$s = \sqrt{s^2} = \sqrt{\frac{1}{n-1}\sum_{i=1}^{n} (y_i - \bar{y})^2} \tag{3.8}$$

Where n is the number of observations and $\bar{y}$ is the sample mean. A t-test is used to compare the conversions between different temperatures. The t-test is based on the t-distribution, which is given by the following formula:

$$f(y) = \frac{\Gamma\left(\frac{\nu+1}{2}\right)}{\Gamma\left(\frac{\nu}{2}\right)\sqrt{\pi\nu}}\left(1+\frac{y^2}{\nu}\right)^{-(\nu+1)/2} \tag{3.9}$$

Where $\nu = n-1$ is referred to as the degrees of freedom **[23]**. All t-distributions possess a bell shape, similar to the normal distribution, and the t-distribution becomes almost identical to the normal distribution when n>30. T-tests for independent samples can be carried out assuming that the variances are equal as well as unequal.

The t-test carried out to test whether the conversions differ across temperatures is based on the assumption that the means have unequal variances. A null as well as an alternative hypothesis are chosen, with the null hypothesis stating that the means of the two populations are equal, whereas the alternative hypothesis states that the means differ. The significance level, α or confidence level of the test is then decided. The significance level determines

whether the t-test is single sided or two sided. In the case of a two-sided test being used, the significance level is given by $\alpha/2$. The t value is then calculated using the following formula:

$$t = \frac{\bar{y}_{1.} - \bar{y}_{2.}}{\sqrt{\frac{s_1^2}{n_1} + \frac{s_2^2}{n_2}}} \tag{3.10}$$

Where n_1 and n_2 are the sample sizes and s_1 and s_2 are the variances of the two populations. The calculated t value is then compared to a critical t value obtained from statistical tables **[23]**. The critical t value is obtained based on the significance level of the test and the approximate degree of freedom that is calculated from the following formula:

$$df = \frac{\left(\frac{s_1^2}{n_1} + \frac{s_2^2}{n_2}\right)^2}{\frac{1}{n_1 - 1}\left(\frac{s_1^2}{n_1}\right)^2 + \frac{1}{n_2 - 1}\left(\frac{s_2^2}{n_2}\right)^2} \tag{3.11}$$

Where n_1 and n_2 are the sample sizes from the two populations. If the t calculated > t critical the means are said to differ and the null hypothesis is rejected, whereas if t calculated < t critical the means do not differ and the null hypothesis is accepted **[23]**.

3.2 Ash Selection

The ash produced by fluidized bed combustion is of two types. Bed ash is the excess material that remains in the bed and consists of coal-derived ash, tramp material fed with the coal, inert bed material like silica sand and CaO and $CaSO_4$. Bed ash particles are usually ~1 mm and their size depends on coal particle size distribution and the selected nominal size of the inert material. Bed ash is removed from the bottom of the bed **[3]**. Fly ash is separated from the flue gas by baghouse filters or electrostatic precipitators and mainly consists of fuel ash, limestone-derived residues (mostly CaO and $CaSO_4$) and unburned carbon or char from the fuel.

Tests here are carried out using four bed ashes from three different sources. Two of the bed ashes, which differ in age, are from the Nova Scotia Power 183 MWe CFBC. The aged ash was obtained in 2001 while the fresh ash was received in June 2005. The other two ashes are from a CFBC at Piney Creek, USA and from the A/C power corporation, USA. The elemental analysis of the four bed ashes is given in Table 3.2.

Table 3.2: Elemental analysis of bed ashes

Test Name	Aged Ash	Fresh Ash	Piney Creek	A/C power
SiO_2	5.18 wt%	4.78 wt%	28.51 wt%	40.87 wt%
Al_2O_3	1.42 wt%	1.2 wt%	9.72 wt%	13.75 wt%
Fe_2O_3	0.5 wt%	0.3 wt%	4.95 wt%	3.08 wt%
TiO_2	0.1 wt%	0.09 wt%	0.51 wt%	0.75 wt%
P_2O_5	< 0.03 wt%	< 0.03 wt%	0.122 wt%	0.071 wt%
CaO	49.73 wt%	51.99 wt%	36.51 wt%	26.07 wt%
MgO	0.59 wt%	0.62 wt%	0.83 wt%	1.58 wt%
SO_3	38.87 wt%	35.47 wt%	11.87 wt%	8.44 wt%
Na_2O	<0.20 wt%	< 0.20 wt%	<0.200 wt%	<0.200 wt%
K_2O	0.19 wt%	0.22 wt%	1.29 wt%	1.52 wt%
Ba	519 ppm	517 ppm	598 ppm	439 ppm
Sr	268 ppm	288 ppm	488 ppm	612 ppm
V	3027 ppm	3087 ppm	62 ppm	83 ppm
Ni	774 ppm	673 ppm	<50 ppm	<50 ppm
Mn	1023 ppm	1037 ppm	692 ppm	65 ppm
Cr	102 ppm	94 ppm	<50 ppm	53 ppm
Cu	70 ppm	69 ppm	42 ppm	30 ppm
Zn	50 ppm	59 ppm	46 ppm	<30 ppm
Loss on Fusion	2.78 wt%	4.7 wt%	5.47 wt%	3.70 wt%
Sum	99.95 wt%	99.95 wt%	99.98 wt%	99.96 wt%
CO_2	0.25 wt%	0.79 wt%	2.12 wt%	0.51 wt%

3.3 Selection of Additives

Two additives were considered for the carbonation reaction, namely sodium chloride and seawater from Nova Scotia. Conditioning the ash with seawater at Point Aconi is a possibility since the plant is located on the Atlantic. It has been shown in literature **[24, 25]** that sodium chloride increases the solubility of Ca ions, thereby increasing the rate of hydration of lime. As the ash must be hydrated prior to being carbonated **[16, 26]** additives like NaCl should increase the hydration rate and possibly also the carbonation rate of the ash. The concentration of NaCl used is 35g/l for all tests in order to simulate the concentration of salt in seawater.

3.4 Operating Conditions

The operating conditions are based on information from previous tests. A water-to-solid ratio of 10:1 was maintained for all tests. This value is somewhat arbitrary, but is based on the assumption that large water to solid ratios would allow better control of the exothermic hydration reaction. The amplitude for the VCX 600 unit is maintained at 50% for all tests and is based on previous work **[26]**, which showed that good conversions were obtained at medium amplitudes. The power delivered to the probe for the VCX 600 unit is found to be around 90-110W. The VCX 750 unit required an amplitude of 90% in order to deliver the same amount of power to the probe. A CO_2 flow rate of 0.1 l/min is maintained for all tests as it provides more than sufficient CO_2 for the carbonation reaction and represents the baseline condition. Tests are carried out for time periods of 5, 10, 15, 20, 40 and 60 minutes for the batch tests. Four different temperatures of 20, 40, 60 and 80°C are used. The semi-continuous tests are carried out at 40, 60 and 80°C.

4. Results and Discussion

The following section presents the experimental results and discussions concerning the temperature dependence, effect of additives and kinetics of FBC ash. The results from TGA and TGA-FTIR, XRD and wet sieving tests are also presented. The results of comparisons carried out between utrasonics and stirring have also been presented.

4.1 Temperature dependency of FBC ash under simultaneous hydration and carbonation.

The conversion to hydroxide of the aged NSPI (Nova Scotia Power) ash at different temperatures is shown in Figure 4.1. It can be seen that the conversion of CaO to $Ca(OH)_2$ decreases as temperature increases. At higher temperatures of 60 and 80°C a sharp decrease in the level of hydration can be observed when compared to lower temperatures of 20 and 40°C when the ash undergoes simultaneous hydration along with carbonation. For example the conversion drops from a value of 69 ± 2% at 20°C to 43 ± 2% at 60°C to a value of 14 ± 1% at 80°C for 15 minutes. A statistical analysis was carried out on the above values by utilizing a t-test considering unequal variances. The null hypothesis tested assumes that the means do not differ. When comparing the conversion to hydroxide between 20 and 60°C a calculated t value of 6.44 is compared to a critical t value of 6.314 with a 90% confidence level (n = 2) **[23]**. As the calculated t value is greater than the critical t the null hypothesis is rejected showing that the means differ, leading to the observation that the conversion to hydroxide decreases with increasing temperature. A t-test is also carried out to test the conversions obtained between 60 and 80°C with t = 10.66 being compared to $t_{\alpha=0.1,\ n=2}$ = 6.314, leading to a rejection of the null hypothesis. The conversion to hydroxide also appears to drop with increasing time as it decreases from a value of 43 ± 2% at 15min to 22 ± 1% at 40min at a temperature of 60°C. These results are statistically significant as t values calculated to test the two conditions gave values of 7.90 and 6.314 for t and $t_{\alpha=0.1,\ n=2}$, respectively.

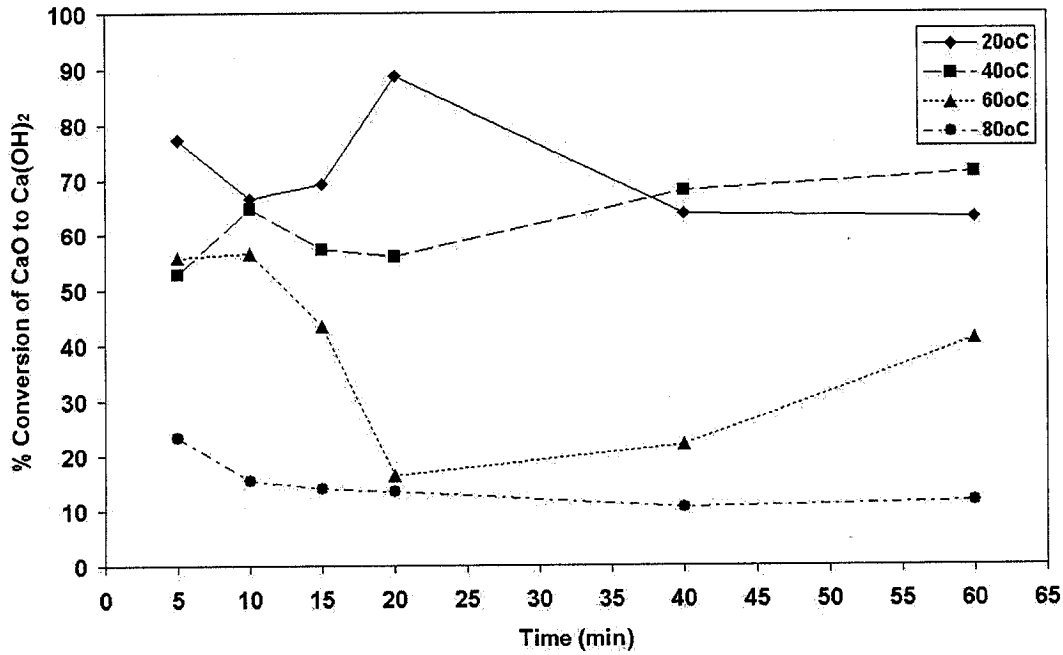

Figure 4.1: Aged ash - comparison of hydration at different temperatures

Figure 4.2 shows the carbonation conversion of the aged NSPI ash at different temperatures. This graph displays the opposite trend to that of hydration as the conversions appear to increase with increasing temperatures. At lower temperatures of 20 and 40°C, modest increases in the level of carbonation are observed while at higher temperatures of 60 and 80°C the rate of carbonation increases significantly. It can be observed that the conversion of CaO to $CaCO_3$ increases from 7 ± 1% at 20°C to 44 ± 1% at 60°C, to a value of 73 ± 5% at 80°C for 15 minutes. When comparing the conversions to carbonate between 20 and 60°C, t of 21.34 versus $t_{\alpha=0.1,\ n=2}$ of 6.314 is obtained showing that the carbonation increases with temperature. Repeat tests were carried out with the aged NSPI ash at a temperature of 80°C for a time period of 20 min using the VCX 750 unit. Hydroxide conversion of 26% and 25 ± 2% were obtained while conversions to carbonate of 74 ± 2% and 68 ± 1% were measured. These values are comparable to earlier values of 15 ± 1% for hydration conversion and 75 ± 5% carbonation conversion that were obtained during the first run with the VCX 600 unit. The pH of the ash water mixture measured prior to sonication was recorded and was found to be in the range of 11-12, indicating the calcic nature of FBC ash. However, the pH of the mixture after simultaneous hydration and carbonation was found to decrease and values in the range of 6-7 were recorded.

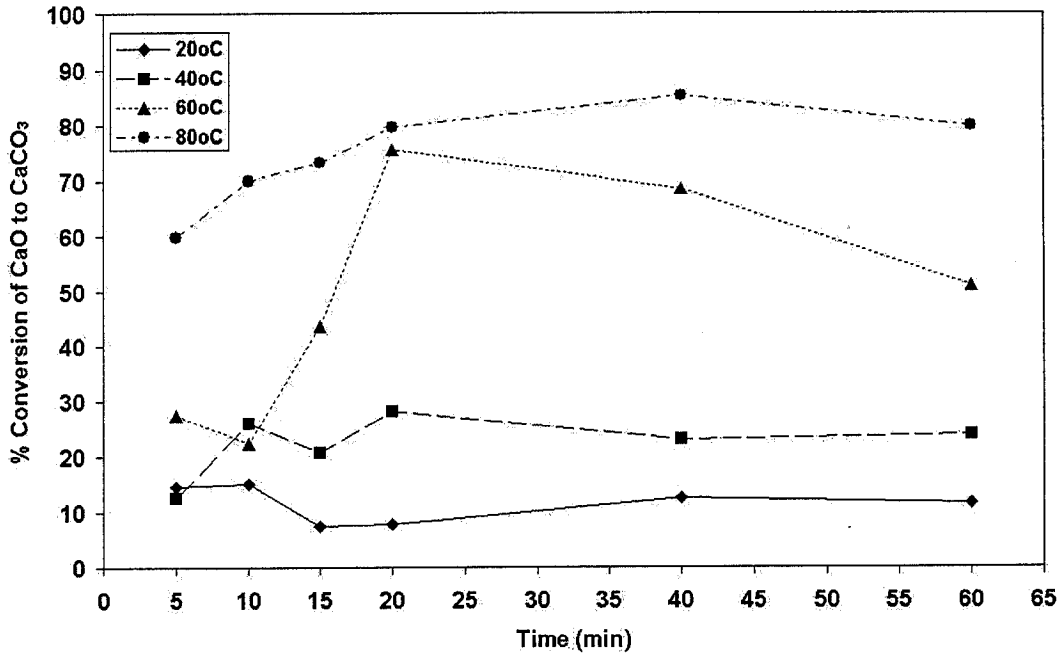

Figure 4.2: Aged ash - comparison of carbonation at different temperatures

When hydration as well as carbonation is considered together it appears that the unreacted CaO undergoes hydration to form $Ca(OH)_2$ which in turn reacts with CO_2 to form $CaCO_3$. A similar trend was also observed by Anthony *et al.* **[26]** when carbonating NSPI bed ashes using ultrasonics. The conversion to $Ca(OH)_2$ appears to decrease with increasing temperature. However, this is not the case as conversions to hydroxide actually increase in the temperature range of 50-80°C when ultrasonics is used **[27]** and the apparent decrease in hydration is due to the carbonation reaction. The reaction mechanism follows that of a consecutive series mechanism and as a result as the rate of the carbonation reaction increases with time and temperature, greater amounts of $Ca(OH)_2$ convert to $CaCO_3$. Hence, a decrease in the conversion of CaO to $Ca(OH)_2$ can be observed.

Figure 4.3 displays the hydroxide conversion of the fresh NSPI ash while Figure 4.4 displays the conversion to carbonate. The fresh ash appears to follow the same trend of decreasing hydroxide conversion followed by an increase in carbonation with increasing temperatures. The conversion to $Ca(OH)_2$ decreases from 74 ± 6% at 20°C to 44 ± 1% at 60°C for 15 min, while the conversion to $CaCO_3$ increases from 15 ± 1% at 20°C to 43% at 60°C for the same

time period. As conversion to carbonate is of greater interest a t-test was carried out to test the validity of the observation statistically. As the t of 15.65 is greater than $t_{\alpha=0.1,\ n=2}$ value of 6.314, an increase in the conversion to $CaCO_3$ with increasing temperatures is seen for the fresh ash as well. Table 4.1 shows the overall conversion of the fresh NSPI ash to product. High overall conversions of 101% at 40°C, 60 min and 108% at 80°C, 10 min can be observed from the table. Conversions greater than 100% for two different ashes had also been previously observed [27]. The reason for these values is most likely the participation of OCC in the reaction. Anthony *et al.* [28] have shown the existence OCC like gehlenite, larnite and di-calcium ferrite in FBC ash and suggested the possibility of excess CaO being provided by these compounds for the carbonation reaction.

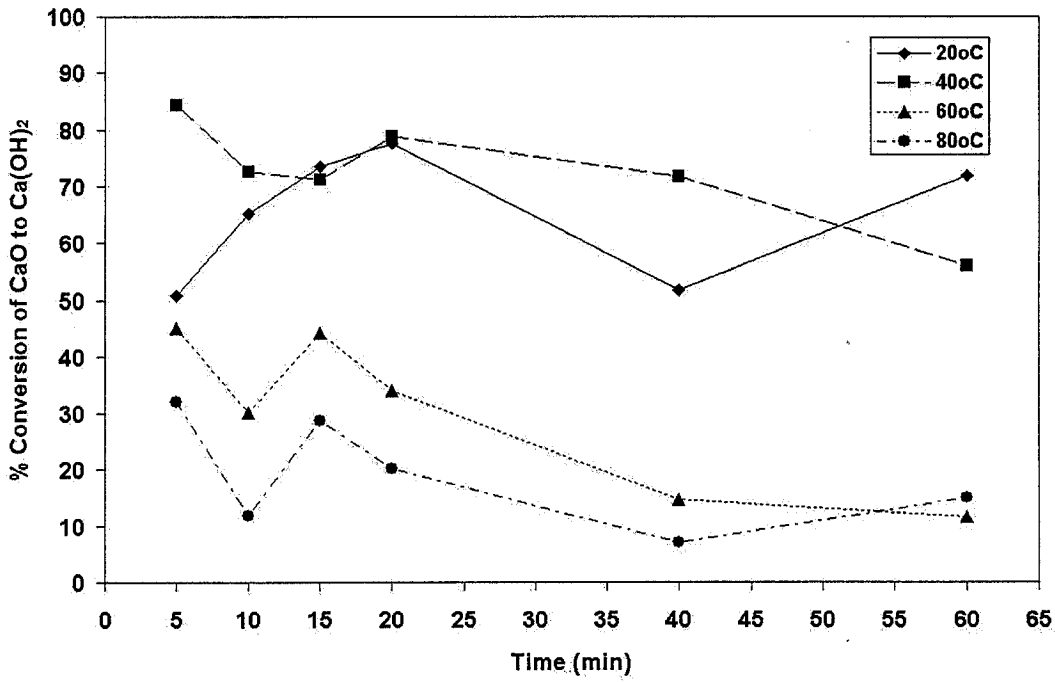

Figure 4.3: Fresh ash - comparison of hydration at different temperatures

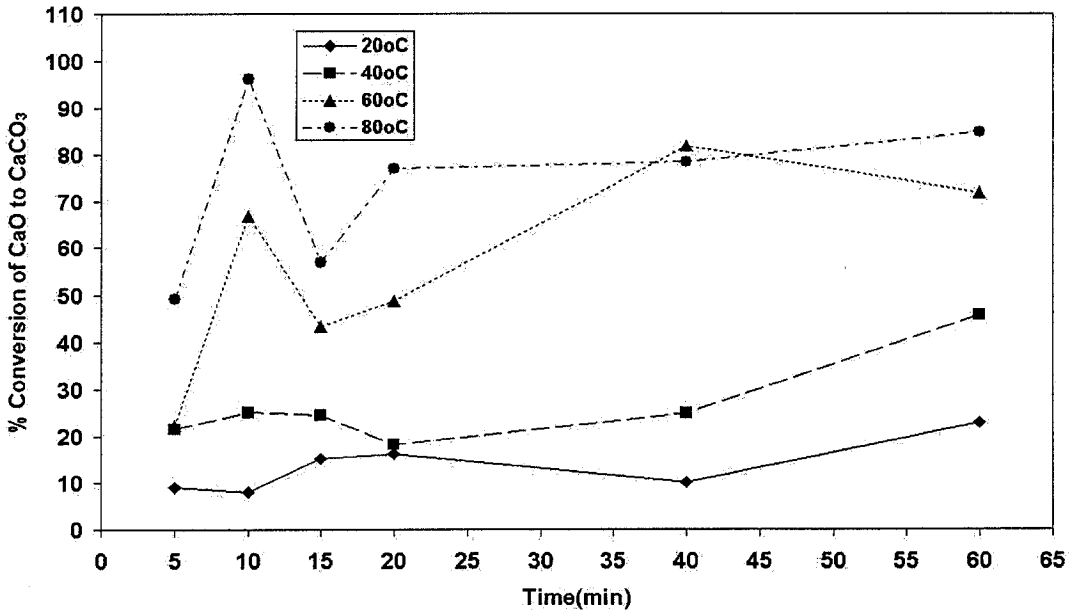

Figure 4.4: Fresh ash - comparison of carbonation at different temperatures

Table 4.1: Overall conversions of CaO to carbonate and hydroxide for fresh ash

Time (min)	% Overall Conversion, 40°C	% Overall Conversion, 80°C
5	106	81
10	98	108
15	96	86
20	97	97
40	97	85
60	102	100

Figures 4.5 and 4.6 display the conversion of the fresh ash to hydroxide and carbonate from the tests using semi-continuous sampling. From Figure 4.5 it can be seen that the conversion to hydroxide decreases with time as well as temperature and displays the same trends exhibited by the conversions obtained from the batch tests. From Figure 4.6 it can be seen that the conversion to carbonate increases between 0 to 10 minutes after which it remains at an almost constant value and begins to increase after 20 minutes. This trend can be observed

across all three temperatures tested. The data obtained from the semi-continuous sampling tests are comparable in magnitude to those from the batch tests.

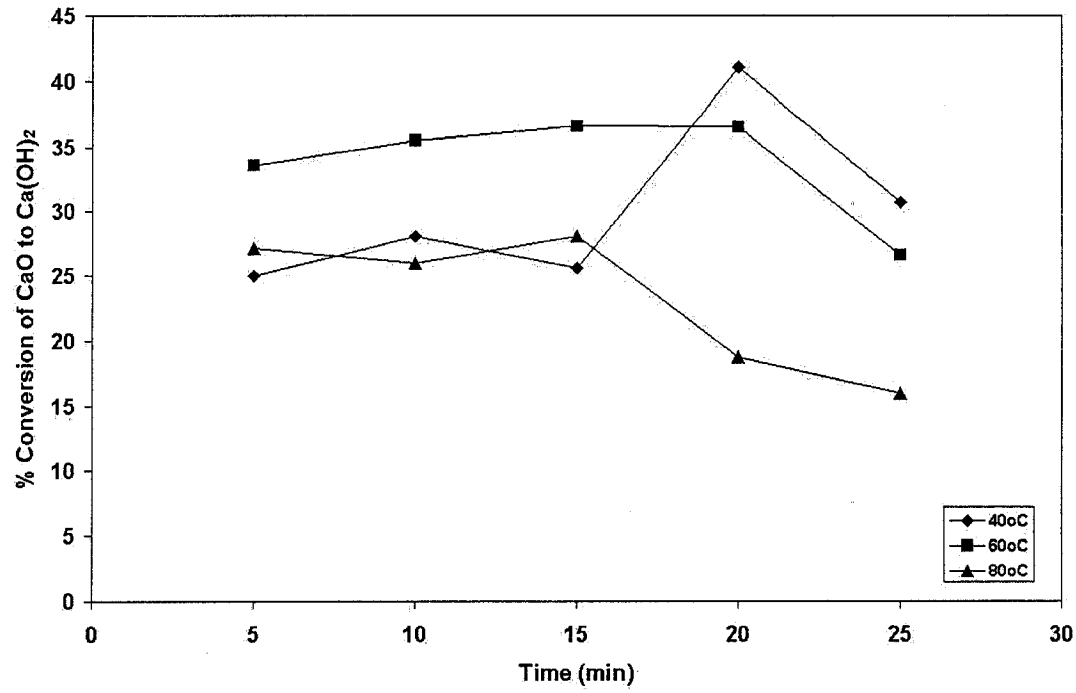

Figure 4.5: Fresh ash – comparison of hydration, semi-continuous sampling method

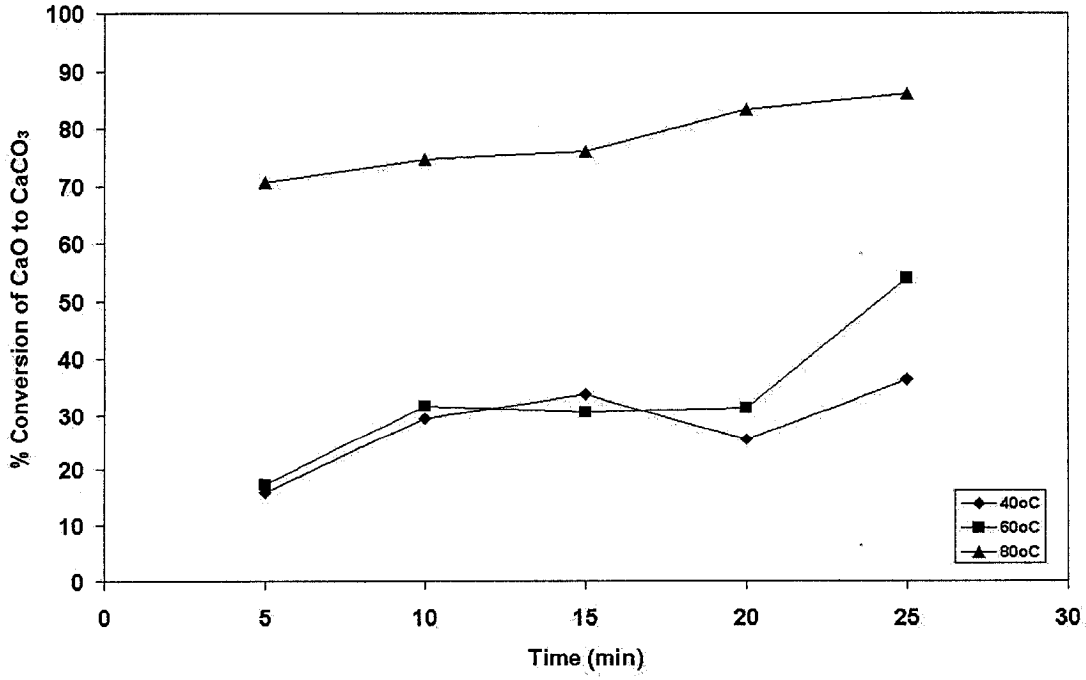

Figure 4.6: Fresh ash – comparison of carbonation, semi-continuous sampling method

4.2 Effect of additives on hydration and carbonation of FBC ash.

Figure 4.7 and 4.8 show the effect of additives on the conversion of CaO to $Ca(OH)_2$ and conversion of CaO to $CaCO_3$ for the aged NSPI ash. Increase in the conversion of CaO to $Ca(OH)_2$ when additives are used can be observed from Figure 4.7. With NaCl as additive the conversion to hydroxide increases to 61 ± 5% as compared to 43 ± 2% for the ash without additive for a time period of 15min. Similarly, seawater appears to increase hydration levels in the ash when used as an additive, as a value of 69 ± 5% is observed for the aged ash with seawater as additive. Statistical analysis indicates that the means do not differ when comparing the aged ash to the ash sonicated with additives. The t values of 2.32 and 3.54 are lower than $t_{\alpha=0.1, n=2}$ value of 6.314 indicating that the means do not differ.

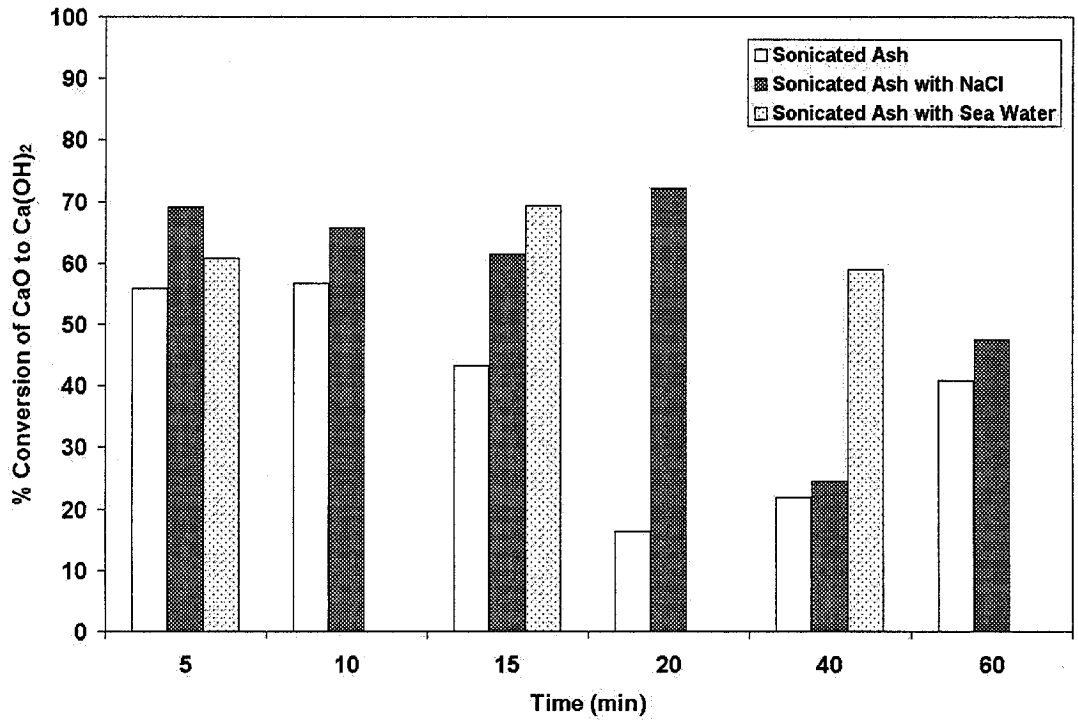

Figure 4.7: Effect of additives on hydration - aged ash at 60°C

The effect of additives on the conversion to carbonate is given in Figure 4.8. The additives do not positively affect the carbonate conversion of the aged NSPI ash. For example the conversion to carbonate for the aged ash with NaCl as additive is 21 ± 4% as compared to 44 ± 1% for the aged ash without additive for a time period of 15min. A similar trend is also observed when comparing the aged ash with seawater as additive to the aged ash without

additives with values of 28% for the ash with seawater. A statistical t-test confirms the above observation with the t value of 10.67 being greater than the $t_{\alpha=0.1, n=2}$ value of 6.314 leading to a rejection of the null hypothesis showing that the conversion to carbonate is higher for the aged ash without seawater as additive. The fresh ash with additives also displays the trends exhibited by the aged ash with additives. The hydration levels of the fresh ash increase when NaCl and seawater are used as compared to the ash without additives. High hydration levels of the ash when sonicated for time periods of 40min or longer have been observed when additives are used which again suggests incomplete carbonation.

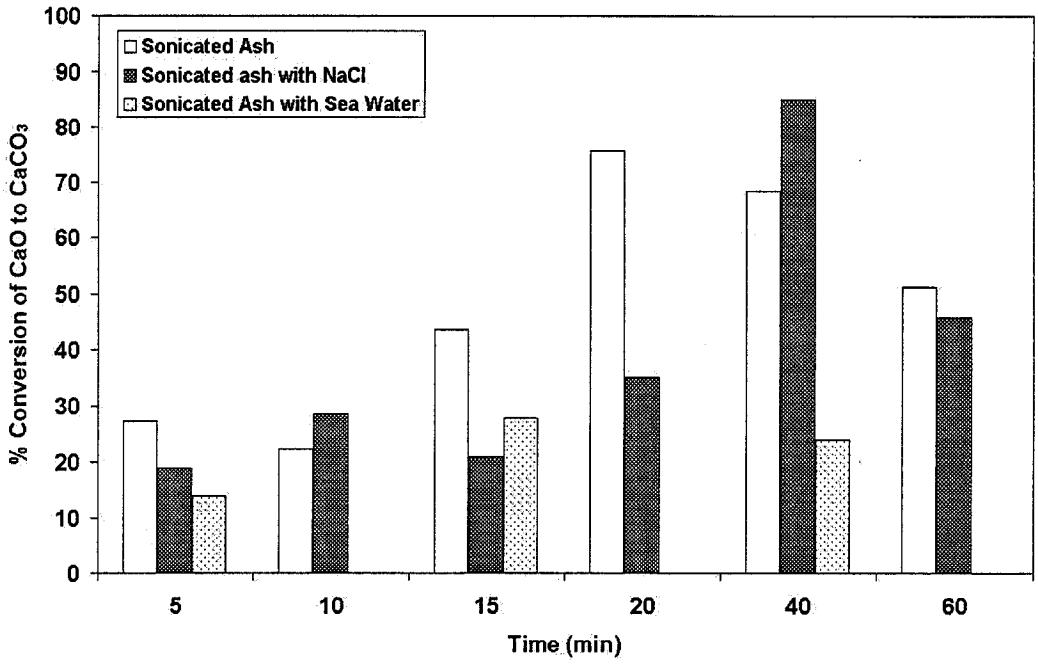

Figure 4.8: Effect of additives on carbonation - aged ash at 60°C

4.3 Rate constants and activation energy of the carbonation reaction

The rate constants for the carbonation reaction are obtained from the plots of conversion *versus* time for the aged as well as fresh NSPI ash and are shown in Figures 4.9 and 4.10. The reaction is assumed to be first order with respect to calcium oxide concentration. Both the plots show a fair amount of scatter, which is due to experimental

error as well as the variance associated with the batch nature of the tests. The rate constants are shown in the graphs for all temperatures tested. The magnitude of the rate constants appears to increase with increasing temperature indicating the temperature-dependent nature of the reaction. The activation energy for both ashes is obtained by plotting the rate constant *versus* temperature and is shown in Figures 4.11 and 4.12. Similar graphs were also plotted for the aged as well as fresh ash with additives. The activation energy of the aged ash obtained from the experimental data is 40 kJ/mol while the activation energy for the aged ash with NaCl as additive is 32 kJ/mol. Similarly, the activation energy of the fresh ash without and with NaCl is 32 kJ/mol and 22 kJ/mol.

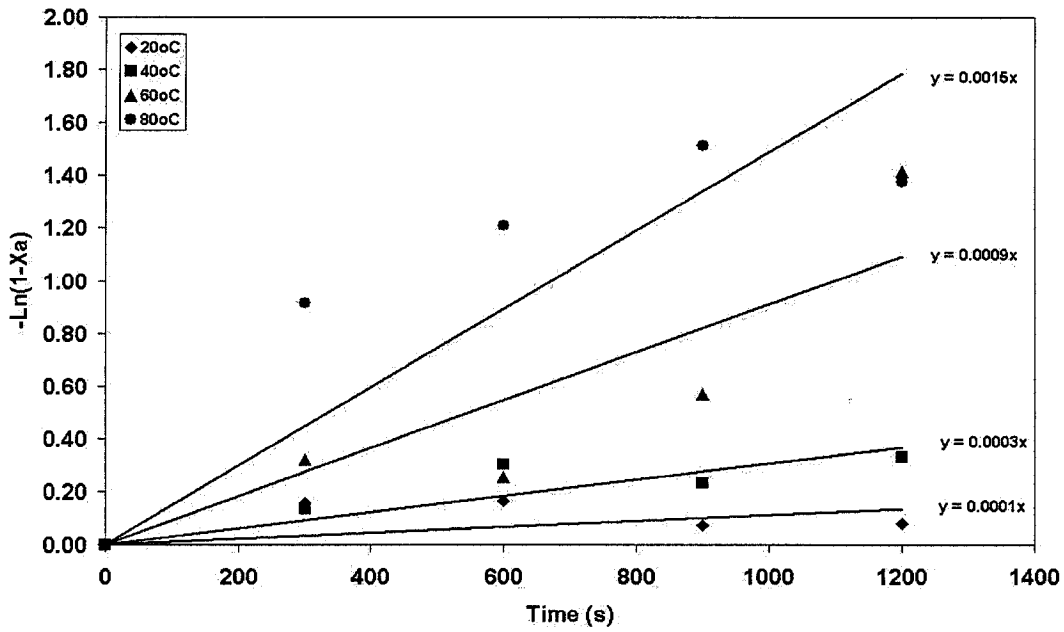

Figure 4.9: Conversion *vs.* time, 1st order reaction – aged ash

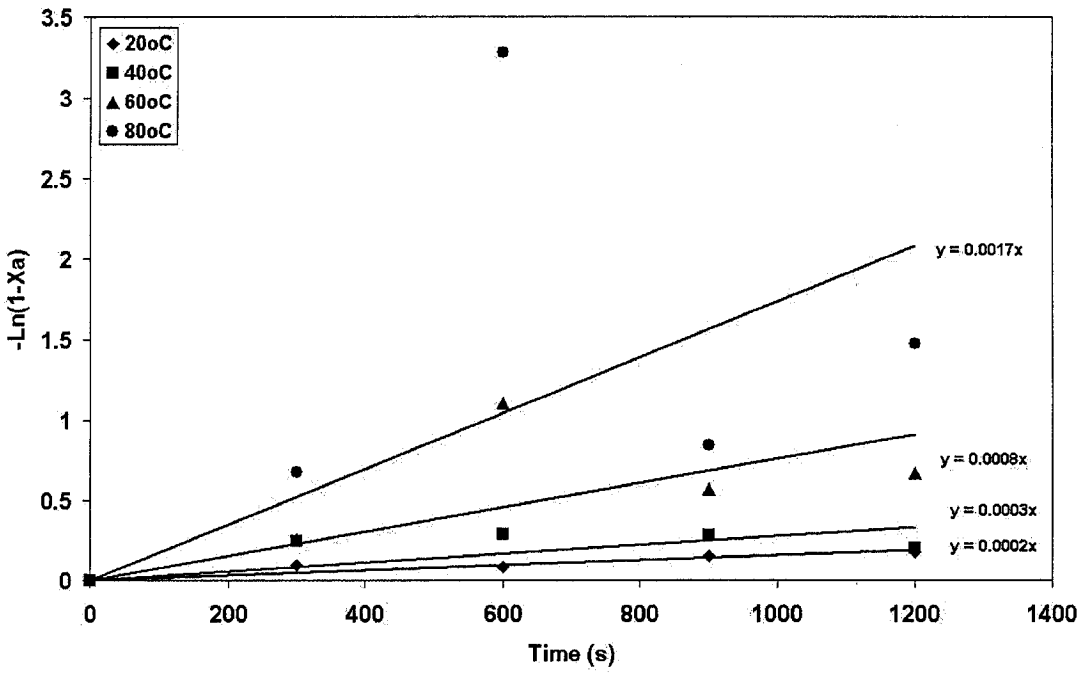

Figure 4.10: Conversion *vs.* time, 1st order reaction – fresh ash

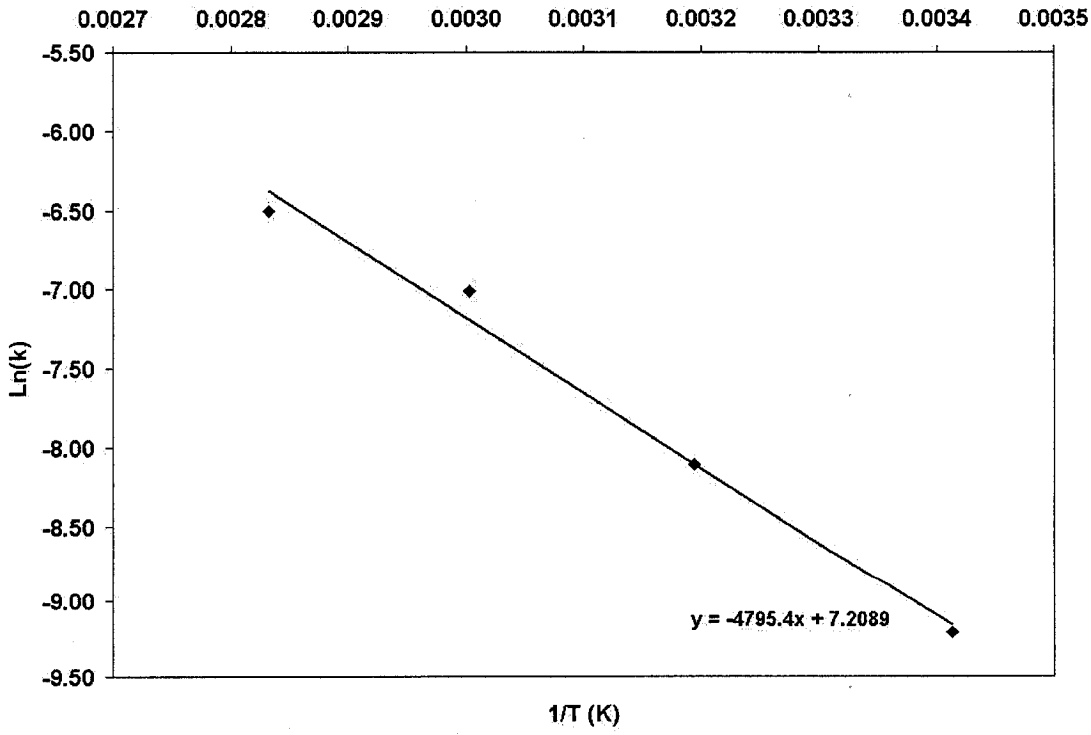

Figure 4.11: Activation energy, 1st order reaction – aged ash

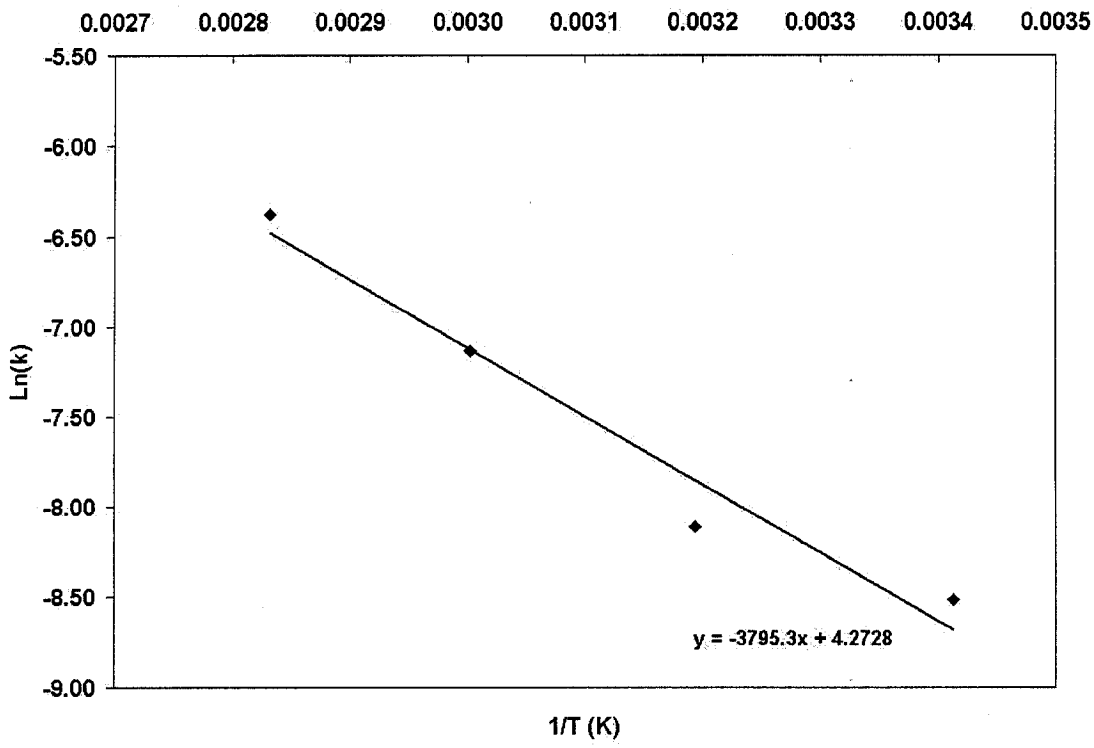

Figure 4.12: Activation energy, 1st order reaction – fresh ash

Figure 4.13 displays the plot of conversion *versus* time for the semi-continuous sampling method. The semi-continuous sampling method was carried out in order to decrease the experimental error as well as the variance in the results of the batch tests. The magnitude of the rate constants increases with temperature and displays the temperature dependency of the reaction. Figure 4.14 displays the plot of the rate constant *versus* time for the continuous process and the activation energy obtained from experimental data is 36 kJ/mol. However the semi-continuous sampling method also displays a reasonable amount of variation and this could be due to the participation of OCC during the reaction.

The kinetics of the batch as well as the semi-continuous sampling method has been approximated using a first order reaction. However on observing the plots of conversion versus for both the fresh as well as aged NSPI ash reveal that the kinetics deviate's from the first order reaction model. Considering that the ash does not carbonate without prior hydration a consecutive series reaction model, given by equation 4.1 could be considered.

$$CaO + H_2O \rightarrow Ca(OH)_2 + CO_2 \rightarrow CaCO_3 \qquad (4.1)$$

Future work focused on obtaining the kinetics of the process could utilize the above reaction model and in order to eliminate the variation caused by the participation of OCC, synthetic sorbents i.e. pure CaO sulphated to different levels could be used.

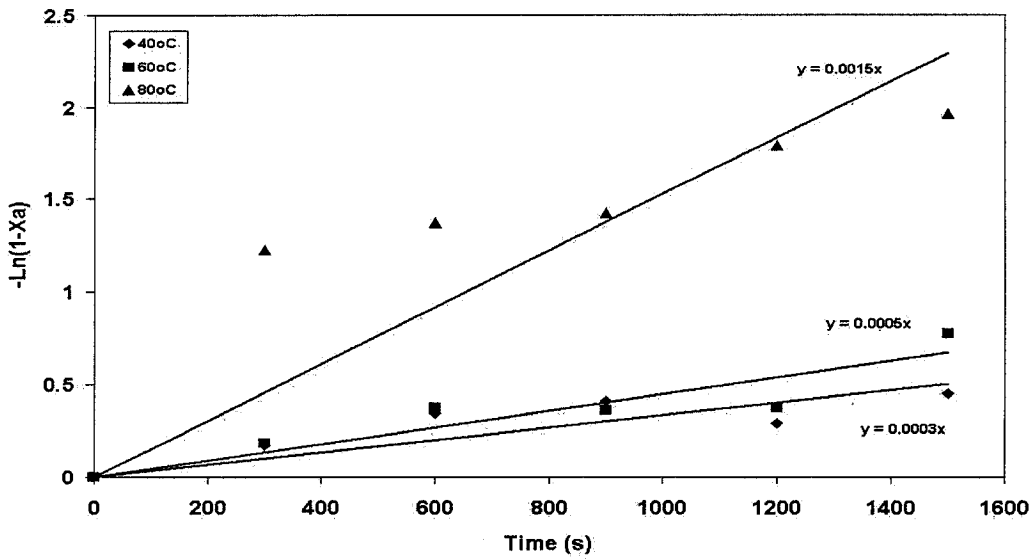

Figure 4.13: Conversion *vs.* time, 1st order reaction – fresh ash, semi-continuous sampling method

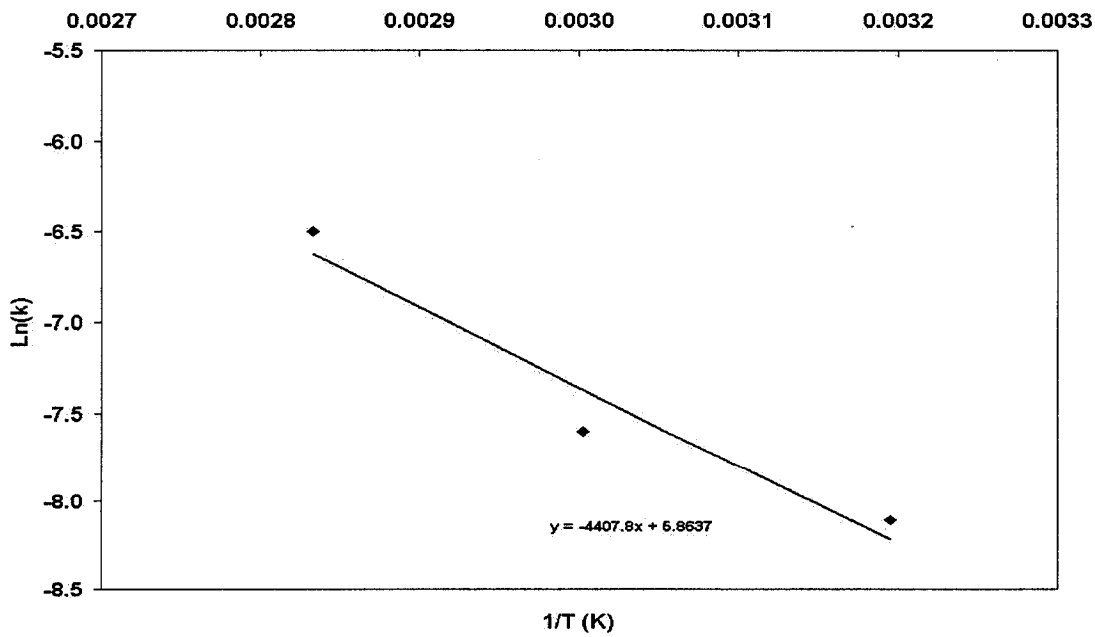

Figure 4.14: Activation energy, 1st order reaction – fresh ash, semi-continuous sampling method

4.4 Comparison between ultrasonics and stirring

Comparisons between stirring and ultrasonics for the aged and fresh NSPI ash are seen from Figure 4.15. The conversions reported here have been obtained by oven tests. The ability of ultrasonics to increase the rate of the carbonation reaction of the aged NSPI ash is seen from Figure 4.15. The conversion to carbonate for the aged ash increases from 62 ± 4% at 15min to 83 ± 6% at 40min and 60°C when ultrasonics is used, whereas when stirring is utilized, the conversion to carbonate displays values of 23 ± 1.5% at 15min and 27 ± 2% at 40min at a temperature of 60°C. A statistical comparison between ultrasonics and stirring shows that the conversions to $CaCO_3$ obtained with ultrasonics are higher than those obtained using stirring. When comparing ultrasonics to stirring at 60°C and 15min, the t value of 6.89 is greater than $t_{\alpha=0.1,\ n=3}$ of 2.92 leading to the conclusion that the means differ. The above result holds good even when comparing longer durations of 40min, with the t value of 5.91 being greater than the $t_{\alpha=0.1,\ n=3}$ value of 2.92. When considering hydration, the values for the aged ash appear to be greater for the experiment where stirring replaces ultrasonics. However, higher conversion to hydroxide is expected due to low carbonate conversion. The hydration of the aged ash also appears to increase with time when compared to the TGA values. However, the values obtained by the TGA test are more accurate as the tests are carried out in an inert atmosphere of nitrogen and can allow us to avoid the effects associated with decomposition of hydrated amorphous silica compounds **[20]**. Fresh NSPI ash shows the same trends as the sonicated ash when subjected to stirring. Higher conversions to carbonate can be observed when stirring the ash for longer time periods and seem to indicate that the fresh ash carbonates to a greater extent than the aged ash. These tests also indicate that ultrasonics is effective in allowing CO_2 access to the unreacted CaO core.

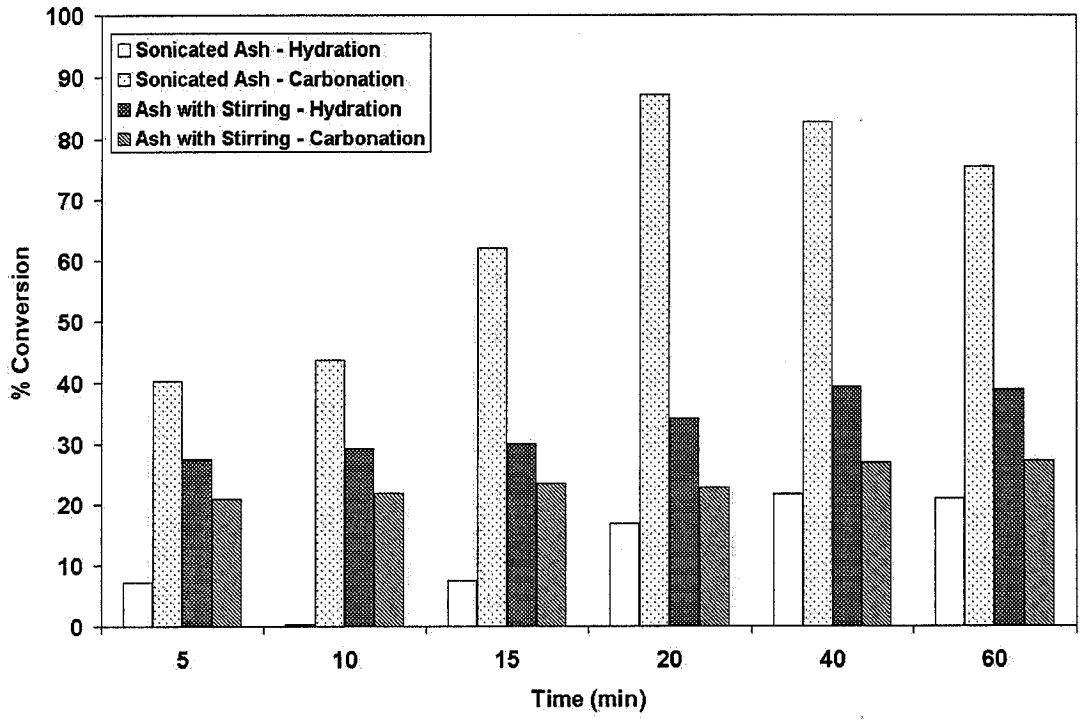

Figure 4.15: Comparison of ultrasonics with stirring - aged ash at 60°C

4.5 TGA and TGA-FTIR analysis of FBC ash

The TGA curves for the fresh NSPI ash are shown in Figure 4.16. Curve 1 in Figure 4.16 displays the weight loss with respect to time for the fresh NSPI ash sonicated at 40°C for a period of 60min. The curve displays a double step weight loss obtained due to the decomposition of both $Ca(OH)_2$ and $CaCO_3$. The first weight loss corresponds to the decomposition of $Ca(OH)_2$ while the second weight loss is due to the decomposition of $CaCO_3$. Curve 2 shows the weight loss for the fresh ash sonicated at 80°C and for a time period of 60min. Curve 2 does not display the double step weight loss and instead displays a gradual weight loss between 100-450°C. The decomposition temperature of $Ca(OH)_2$ is known to be in the range of 350-450°C. Gora *et al.* **[29]** have also observed similar results for the steam reactivation of bed and fly ashes. However, the weight loss due to decomposition of $CaCO_3$ is clearly defined. The aged ash along with the bed ashes from Piney Creek and A/C power, USA also display the same effect at higher temperatures. The gradual weight loss displayed by the sample sonicated at 80°C was anomalous and in order to investigate this effect a TGA-FTIR analysis of the sample was carried out.

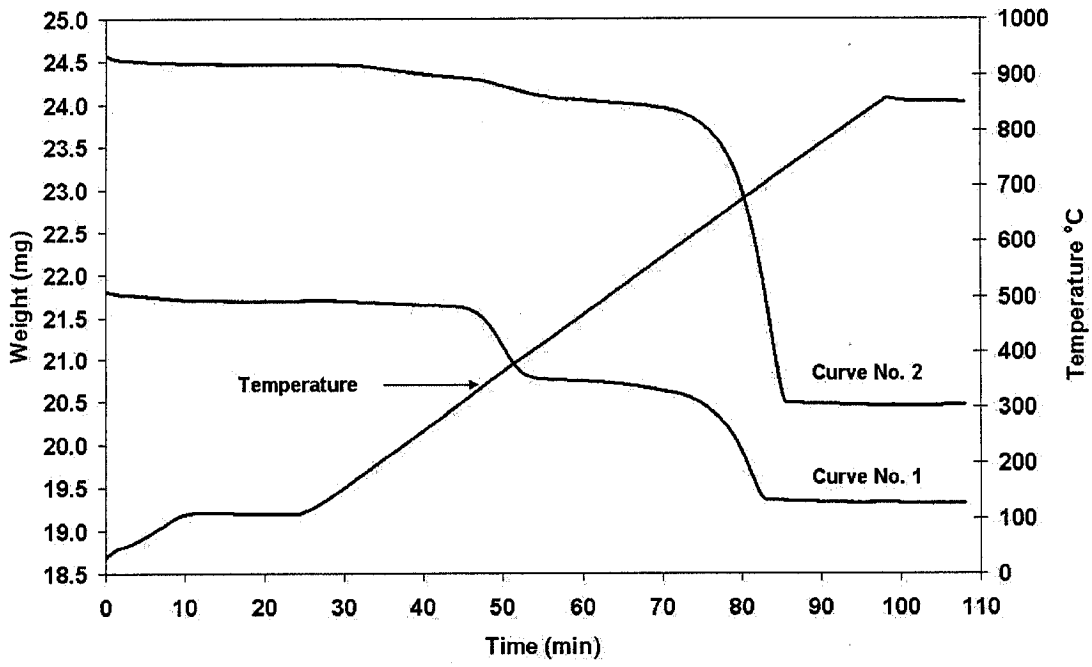

Figure 4.16: TGA curves - fresh ash sonicated at 40 and 80°C, 60 min

The TGA-FTIR tests were conducted to determinate the rate of evolution, temperature of evolution and composition of the gases being evolved. Figure 4.17 shows such a curve for the fresh ash sonicated at 80°C, 60min and it can be seen that the gases produced are H_2O and CO_2. Water is evolved between 0-170°C, 230-350°C and between 350-460°C and CO_2 evolution takes place between 550-750°C. TGA curves similar to Figure 4.16, curve 2 have also been obtained by Biffen **[30]** when heating calcium silicate hydrates with varying amounts of $Ca(OH)_2$. He observed gradual weight loss between 375 and 650°C when using varying amounts of $Ca(OH)_2$ along with calcium silicate hydrates. Similar results were also observed by Taylor **[20]** when hydrating Portland cement paste. He attributed the gradual weight losses below the decomposition temperature of $Ca(OH)_2$ to the decomposition of amorphous calcium silicate hydrates as well as AFm (Al_2O_3 - Fe_2O_3 - mono) phases. The general formula of the above phase is given by $[Ca_2(Al,Fe)(OH)_6].X.xH_2O$, where X could be one of several anions like OH^-, SO_4^{2-} and CO_3^{2-} for portland cement hydration. The presence of these phases can be observed from the XRD analysis of the sonicated aged and fresh ash. An important implication of these results is that oven tests used to determine the degree of hydration can be seriously in error. It can also be rather difficult to determine the degree of hydration of CaO using TGA. Alternatively expressed, the commonly made assumption in

the FBC literature that in the absence of hemihydrate and gypsum, $Ca(OH)_2$ is the only source of water from such ashes dried above 100°C, is clearly shown to be false.

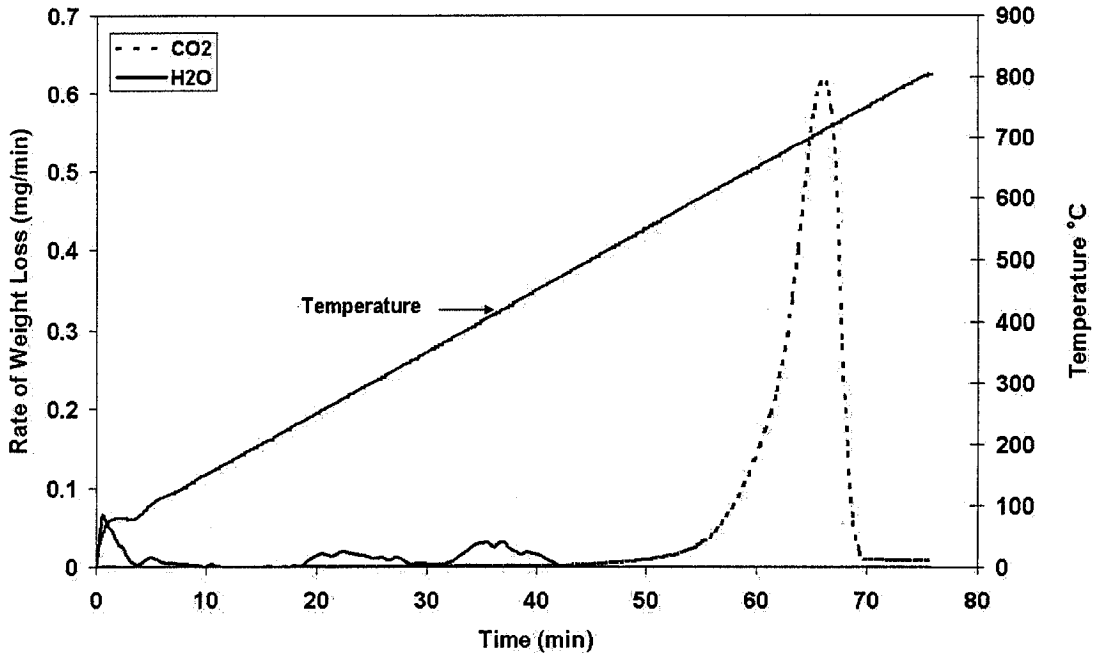

Figure 4.17: TGA FTIR curve - fresh ash sonicated at 80°C, 60 min

Figure 4.18 shows the TGA- FTIR curve for the aged ash sonicated at 80°C and 60min. From this graph it can be seen that water is evolved between temperature ranges of 375-450°C and the water loss is attributed to the decomposition of $Ca(OH)_2$. The water loss between 230-350°C is absent. Figure 4.19 shows the TGA-FTIR curves of the aged NSPI ash sonicated at 20°C, 10min and 40°C, 20min, respectively. The sample sonicated at 20°C shows water losses between 0-150°C and 330-470°C and displays a step in the CO_2 curve between 500-630°C. An XRD analysis of the sample indicated the presence of aragonite, which is an orthorhombic form of calcite. Aragonite is unstable and tends to transform into calcite in the presence of moisture without any change in chemical composition **[24]**. The presence of aragonite indicates the complexity of the process. The sample sonicated at 40°C shows gradual water loss between 0-290°C and could indicate that hydrated calcium silicate hydrates, and as well that AFm (Al_2O_3 - Fe_2O_3 - mono) phases could be decomposing. The temperature-dependent nature of the process can be seen by comparing the two FTIR curves for the aged ash. The aged ash sonicated at higher temperature evolves a greater amount of CO_2 when compared to the aged ash sonicated at 20°C. When comparing the FTIR curves for

the aged ash at three temperatures of 20, 40 and 80°C it can be clearly seen that as temperature increases, the level of hydration decreases with a corresponding increase in the level of carbonation.

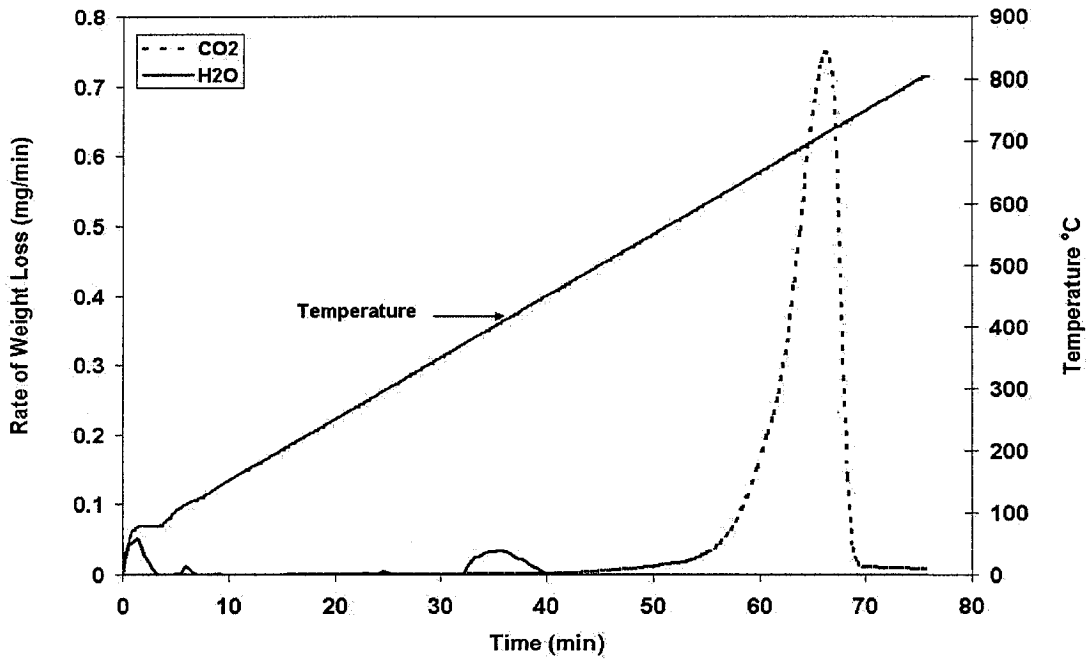

Figure 4.18: TGA FTIR curve - aged ash sonicated at 80°C, 60 min

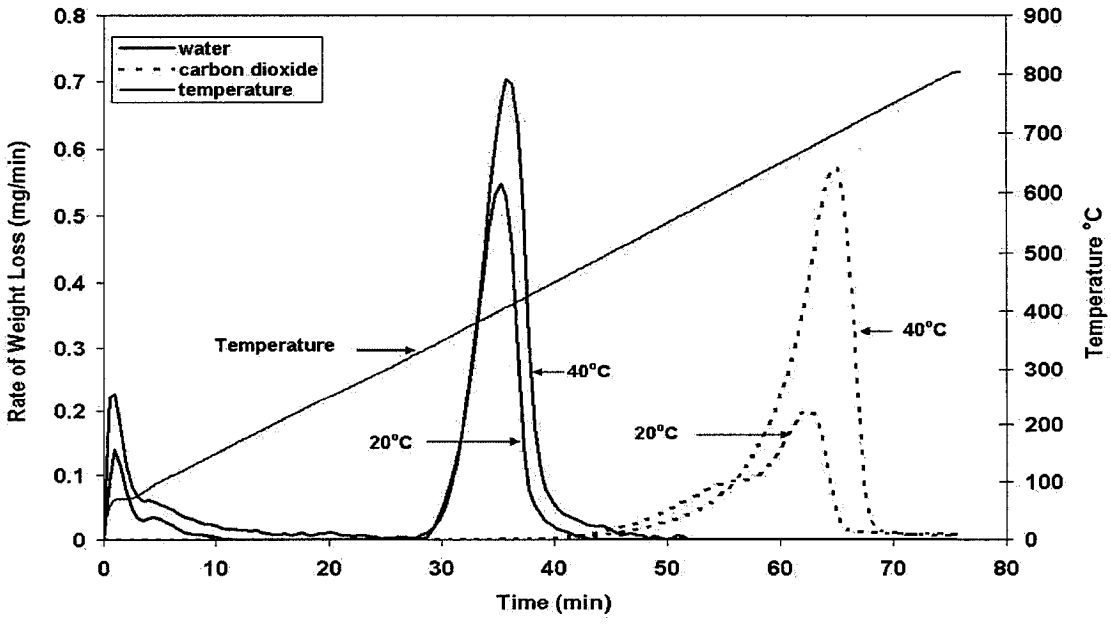

Figure 4.19: TGA FTIR curves - aged ash sonicated at 20, 40°C

4.6 XRD (X ray diffraction) analysis of FBC ash

XRD analyses of the fresh and aged NSPI bed ash are shown in Table 4.2. From the table it can be seen that calcium sulphate is the major constituent of both ashes. The aged ash appears to be sulphated to a greater extent than the fresh ash, with 66% of the ash appearing as calcium sulphate as compared to 62% for the fresh ash. Greater quantities of quartz are present in the aged ash as compared to the fresh ash. The available free lime, CaO + $Ca(OH)_2$, expressed as CaO, for the aged ash is 21.2% while the fresh ash contains 23.5%. The XRD analysis of the amount of available free lime is comparable to the modified ASTM C25 free lime test that gave values of 18 ± 1% for the aged ash and 22 ± 1% for the fresh ash. The aged ash shows a greater amount of portlandite ($Ca(OH)_2$) when compared to the fresh ash. However, this result is to be expected as CaO displays a strong tendency to react with water.

Table 4.3 displays the XRD analyses of the aged and fresh NSPI ash sonicated at 80°C, 60min. the XRD analyses clearly display the presence of OCC in the form of cebollite ($Ca_5Al_2(OH)_4Si_3O_{12}$), a calcium aluminosilicate and grossular hydroxylian ($Ca_3Al_2(SiO_4,CO_3,OH)_3$). The fresh ash does not display the presence of cebollite; however, grossular hydroxylian is apparently present in both ashes. The fresh ash also displays a greater percentage of calcite (21%) when compared to the aged ash (19%). These results indicate an almost complete conversion of CaO to $CaCO_3$ in both ashes. Very small quantities of portlandite are observed in both ashes.

Table 4.4 displays the XRD analysis of the fresh ash when sonicated with NaCl as an additive and shows the same speciation as the fresh ash. However, the value for the amount of calcite (31%) is greater than the available free lime value by both XRD and free lime analysis. All XRD results indicate the presence of calcium sulphite hydrate. However, these lines are not clearly defined in the XRD pattern and were matched using a computer program, and are most unlikely given the nature of these ashes; therefore, the possibility of a mismatch is highly likely.

Table 4.2: XRD analysis of aged and fresh NSPI bed ash

Chemical Compound	Formula	I/Ic	Aged NSPI Ash		Fresh NSPI Ash	
			Scale factor	% Chemical Compound	Scale factor	% Chemical Compound
Calcium Oxide	CaO	4.3	40.0	10.9	54.6	13.8
Anhydrite, syn	$CaSO_4$	1.75	100.0	66.7	100.0	62.1
Portlandite, syn	$Ca(OH)_2$	1.35	11.9	10.3	12.0	9.7
Quartz, syn	SiO_2	3.6	16.0	5.2	15.0	4.5
Crystallinity (%)				93.1		90.1
Amorphous content (%)				6.9		9.9

Table 4.3: XRD analysis of sonicated aged and fresh ash at 80°C, 60min

Chemical Compound	Formula	I/Ic	Aged NSPI Ash		Fresh NSPI Ash	
			Scale factor	% Chemical Compound	Scale factor	% Chemical Compound
Calcium Sulphate	$CaSO_4$	1.7	100	62.82	100	60.67
Calcite, syn	$CaCO_3$	3.2	56.4	18.82	66	21.27
Portlandite, syn	$Ca(OH)_2$	1.4	2.2	1.68	5.4	3.98
Quartz	SiO_2	3.6	3.8	1.13	2.7	0.77
Cebollite	$Ca_5Al_2(OH)_4Si_3O_{12}$	1	3.5	3.74	-	-
Grossular Hydroxylian	$Ca_3Al_2(SiO_4,CO_3,OH)_3$	2.25	12.8	6.07	3	1.38
Calcium Sulphite Hydrate	$CaSO_3 10.5H_2O$	1.4	4.9	3.74	8.5	6.26
Crystallinity (%)				98		94.33
Amorphous Content (%)				2.01		5.67

Table 4.4: XRD analysis of fresh ash sonicated with NaCl at 80°C, 60min

Chemical compound	Formula	I/Ic	Scale factor	% Chemical Compound
Calcium Sulphate	$CaSO_4$	1.7	98	56.66
Calcite, syn	$Ca(CO_3)$	3.2	100	30.72
Portlandite, syn	$Ca(OH)_2$	1.4	5.1	3.58
Quartz	SiO_2	3.6	4.7	1.28
Grossular Hydroxylian	$Ca_3Al_2(SiO_4,CO_3,OH)_3$	2.25	4.9	2.14
Calcium Sulphite Hydrate	$CaSO_310.5H_2O$	1.4	3.2	2.25
Crystallinity (%)				96.63
Amorphous content (%)				3.37

4.7 Effect of ultrasonics on particle size distribution

Figures 4.20 and 4.21 compare the size distribution of the fresh and aged NSPI ash before and after sonication. The graphs show significant particle size reduction after sonication. From Figure 4.20, 40% of the particles possess a size of less than 20-25μm after sonication as compared to a negligible number of particles for the unprocessed fresh ash. Around 60% of the particles have a particle size lower than 75μm when compared to 7% for the unprocessed ash. The aged NSPI ash also undergoes significant size reduction with 37% of the particles having a particle size of 20-25 μm or lower and 54% of the particles with sizes lower than 75μm as seen from Figure 4.21.

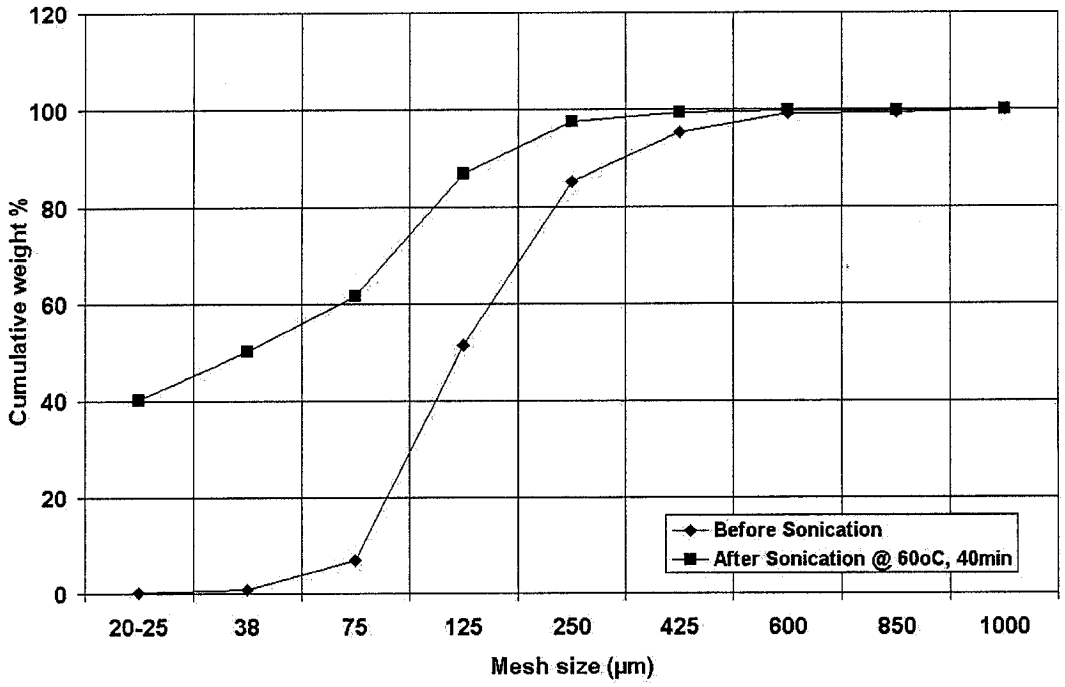

Figure 4.20: Particle size analysis of fresh NSPI ash

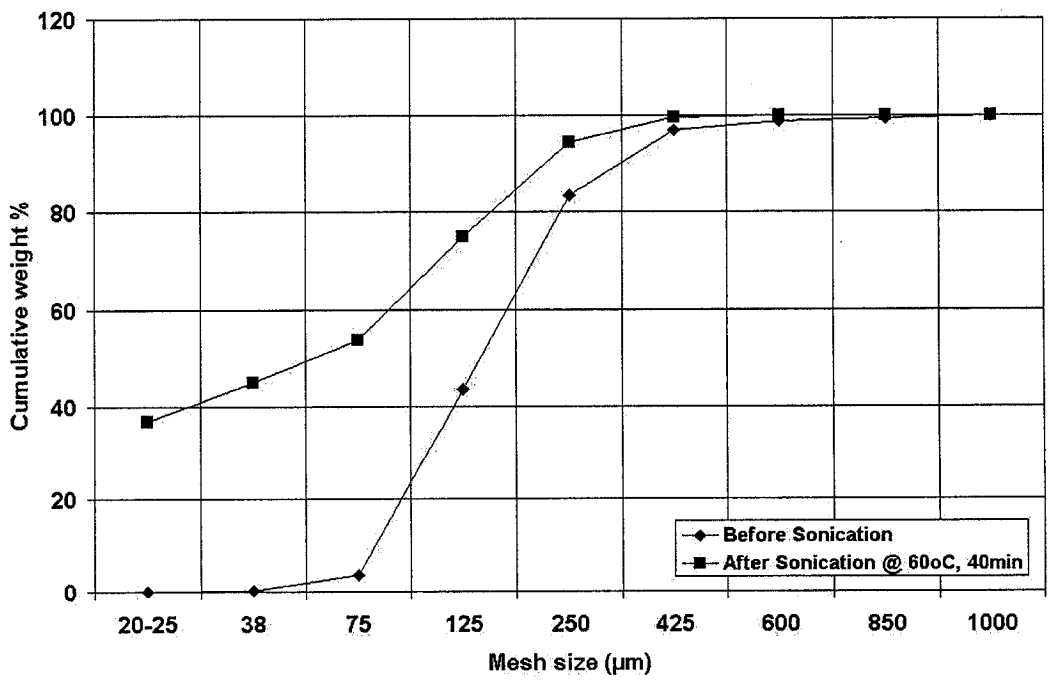

Figure 4.21: Particle size analysis of aged NSPI ash

Figure 4.22 shows the size distribution of the fresh ash which has been sonicated at temperatures of 20, 40 and 60°C for a time period of 40min. Increasing temperatures lead to a decrease in particle size and from the figure it can be seen that 27% of the ash particles have a size smaller than 20-25μm at 20°C as compared to 40% of the particles at 60°C. Over a temperature range of 40°C, the number of particles with a size of 75μm or lower increases from 36% to 60%. Figure 4.23 displays a comparison of the size reduction achieved by ultrasonics and stirring. From the graph it can be seen that ultrasonics is clearly superior to stirring with increasing temperatures yielding higher size reduction when ultrasonics is used. The overall carbonation reaction rate thus increases with an increase in temperature as the intrinsic kinetic rate constant, which follows Arrhenius' Law, is greater and the average particle size is smaller, resulting in exposed CaO and a reduced mass transfer resistance. Loning *et al.* **[31]** have demonstrated that the amount of power delivered into a solution by an ultrasonic probe decreases with increasing temperature. The solubility of CO_2 is also known to decrease with increase in temperature **[32]**. These phenomena would suggest that the carbonation reaction utilizing ultrasonics would benefit from a lower reaction temperature. However, the experimental data clearly indicate the reverse and this can only be explained by the fact that ultrasound is enhancing the carbonation rate due to its size reduction capabilities.

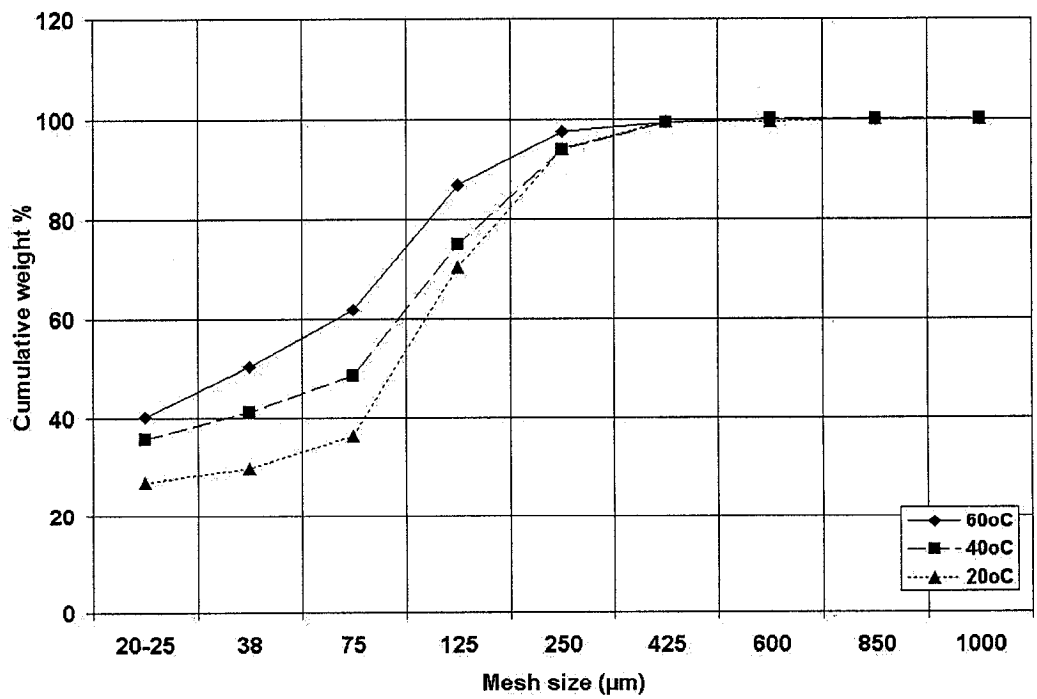

Figure 4.22: Particle size analysis of aged NSPI ash for a sonication period of 40 minutes at three different temperatures.

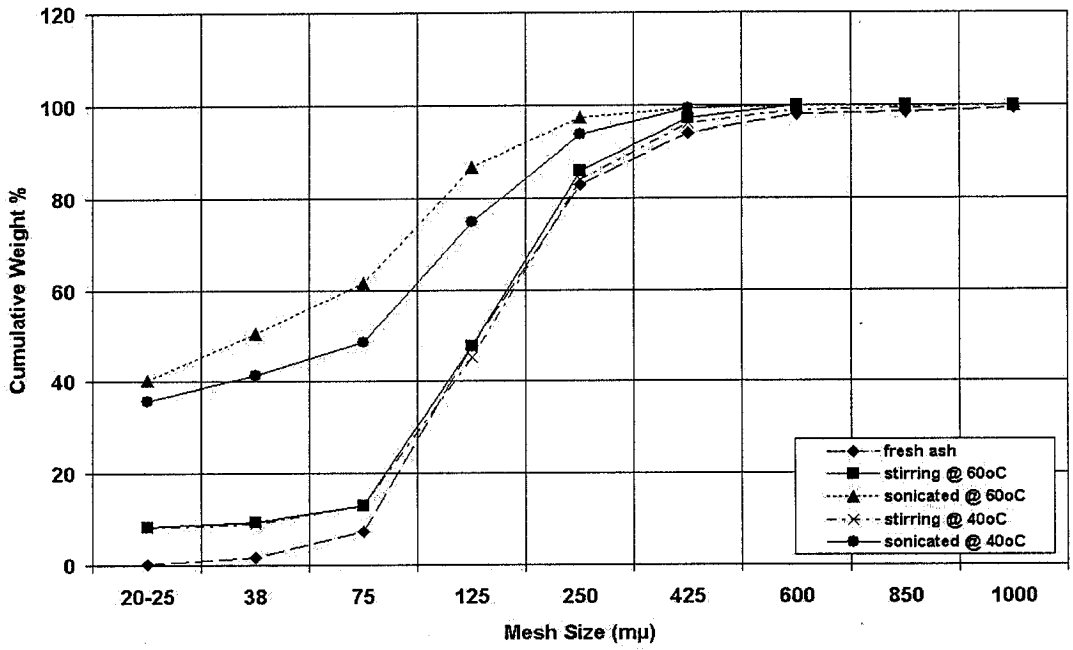

Figure 4.23: Comparison of size reduction between ultrasonics and stirring

4.8 Tests on bed ash from A/C power and Piney Creek

The results of the sonication of bed ashes from A/C power and Piney Creek, USA are presented in Table 4.5. The bed ash from Piney Creek displays moderate conversions to carbonate with values of 54% for 15min and 45 ± 1% for 40min at 60°C. The above results are lower than the values obtained for the NSPI ash. Conversions to hydrate of 31% at 20°C, 15min and 22 ± 1% at 60°C, 15min show the temperature dependency of the ash. The bed ash from A/C power displays conversion levels comparable to the bed ash from Piney Creek. The conversions to carbonate of the bed ash from A/C power are also temperature dependent as conversions increase from 32 ± 2% at 15min, 20°C to 43 ± 1% at 15min, 60°C. The hydration levels of the bed ash from A/C power follow the trends shown by the other three ashes. Ashes from A/C power and Piney Creek were sonicated using the 750W sonicator due to a failure of the older 600W unit and it was found that the higher-rated VCX 750 was unable to deliver sufficient power into the solution at high solution temperatures of 60 and 80°C. When sonicating the samples for longer periods of 40 and 60 min at high temperatures of 60 and 80°C, overheating of the converter was observed. Air-cooling of the converter did not alleviate the problem, which accounts for the low conversions observed in these samples.

However, the repeat tests carried out for the aged NSPI ash at 80°C revealed that the VCX 750 was able to deliver up to 120 Watts at high solution temperatures of 80°C and conversions obtained from these tests were comparable to earlier tests with the VCX 600 unit. This change was brought about by replacing the threaded tip of the probe with a solid tip that is usually used for organic solutions, suggesting that decoupling of the probe from the tip was occurring.

Table 4.5: Conversions of bed ashes from A/C power and Piney Creek

Time	Temperature, °C	Bed Ash from A/C power		Bed Ash from Piney Creek	
		$Ca(OH)_2$, %	$CaCO_3$, %	$Ca(OH)_2$, %	$CaCO_3$, %
15 min	20	49 ± 2	31.5 ± 2	31	45 ± 4
	60	43 ± 3	43 ± 1	22 ± 1	54
40 min	20	53 ± 4	36 ± 8	15 ± 2	45 ± 1
	60	38	50.5 ± 1	24 ± 3	35 ± 3

5. Conclusions and recommendations

1. The tests carried out indicate the temperature dependency for the carbonation of FBC ashes. Temperatures of 60°C and above clearly promote the carbonation reaction and also confirm that carbonation occurs only after the ash has been hydrated.
2. While additives also appear to enhance the hydration reaction, the carbonation reaction does not appear to benefit from their use. Statistical analysis using t-tests confirms the above results.
3. Above stoichiometric conversions of CaO indicate the participation of OCCs. TGA and TGA-FTIR tests along with XRD analysis of the aged as well as the fresh NSPI bed ashes confirm the presence of OCC during hydration as well as carbonation reactions.
4. Due to the complex reaction mechanism the kinetics has been approximated as a first-order reaction and the activation energies of the reaction have been calculated based on experimental results.
5. Wet sieving experiments clearly show the size reduction achieved by ultrasonics and suggest that ultrasonics operate by allowing access to the unreacted calcium oxide. Ashes from three different sources have been tested and demonstrate the general applicability of this technique.
6. Future work will include a more detailed investigation of the kinetics of the carbonation reaction. Current tests have been carried out as a batch process. Future tests need to be conducted so that the conversions can be obtained on a continuous or semi-continuous basis and a more robust model developed for the reaction.
7. The influence of other parameters like water-to-solid ratio as well as the carbon dioxide flow rate could be determined though experiments.
8. Tests comparing ash from industrial FBC with ash prepared synthetically in the laboratory need to be carried out to simplify the analysis and minimize the participation of OCC in the hydration reaction.

Nomenclature

E = activation energy, J/mole

k = rate constant, s^{-1}

k_o = frequency or pre-exponential factor

p_∞ = pressure in liquid far from the bubble, N/m^2

P_A = pressure amplitude

P_o = hydrostatic pressure, N/m^2

$p_L(R)$ = liquid pressure just outside the liquid wall, N/m^2

R, $\check{R}$ = first- and second-order time derivatives of the bubble radius

R = universal gas constant, J/mole °C

s = sample standard deviation

s^2 = sample variance

T = temperature, K

t = time, minutes

$\bar{y}$ = sample mean

X_A = fraction of A converted

Greek symbols

α = significance level of t-test

ρ = density of the fluid, kg/m^3

ω = angular frequency

μ = viscosity in the bulk liquid medium, kg/m s

σ = surface tension of the bulk liquid medium

References

1. S. Rajaram, Next generation CFBC, Chemical Engineering Science, vol. 54, 5565-5571, 1999.
2. E.J. Anthony, Fluidized Bed Combustion of Alternative Solid Fuels: Status, Successes And Problems Of The Technology, Prog. Energy Combust. Sci., vol. 21, 239-268, 1995.
3. Simeon N. Oka, Fluidized Bed Combustion, Marcel Dekker, Inc. New York, 2004.
4. J.P. Longwell, E.S. Rubin and J. Wilson, Coal: Energy For The Future, Prog. Energy Combust. Sci., vol. 21, 269-360, 1995.
5. J R Howard, Fluidized Bed Technology: Principles and Applications, Adam Hilger, Bristol and New York, 1989.
6. P.R. Merriam and J.D. Cousens, Disposal of residue from Nova Scotia Power's 165MWe CFB boiler, Proceedings of the International Conference on Fluidized Bed Combustion, ASME, Vol. 2, 859-865, 1993.
7. Norman Gridley and Desmond Cousens, Nova Scotia Power Corporation Point Aconi Generating Station CFB Residue Management, CANMET Ash Management Seminar, Halifax, Nova Scotia, 1-27, 1991.
8. E.J. Anthony, FBC Waste Disposal: Advanced Ash Disposal Strategies, 49th Purdue Industrial Waste Conference Proceedings, Lewis Publishers, Chelsea, Michigan, 615-620, 1994.
9. Elzbieta M. Bulewicz, Ewa Zoldani, Krystyna Dudek, Final Report on Site Evaluation of the AWDS Process (PERD), CANMET DSS File No. 039SQ.23440-1-9061, 1991.
10. Edward J. Anthony, Robert McCleave, Eduardo Gandolfi, Jinsheng Wang, Industrial scale demonstration of a new sorbent reactivation technology for fluidized bed combustors, Journal of Environmental Management, vol. 69, 177-185, 2003.
11. Rajeev Agnihotri, Shrinivas S. Chauk, S.K. Mahuli, L.S. Fan, Sorbent/Ash Reactivation for Enhanced SO_2 Capture using a Novel Carbonation Technique, Ind. Eng. Chem. Res., vol. 38, 812-819, 1999.
12. L.H. Thompson and L.K. Doraiswamy, Sonochemistry: Science and Engineering, Ind. Eng. Chem. Res., vol. 38, 1215-1249, 1999.
13. Julian R. Frederick, Ultrasonic Engineering, John Wiley and Sons Inc., 1965.
14. Timothy J. Mason, Sonochemistry, Oxford University Press Inc., New York, 1999.

15. Leigh C. Hagenson and L.K. Doraiswamy, Comparison of the effects of ultrasound and mechanical agitation on a reacting solid-liquid system, Chemical Engineering Science, vol. 53, no. 1, 131-148, 1998.
16. L. Jia, E.J. Anthony, Pacification of FBC ash in a pressurized TGA, Fuel, vol. 79, 1109-1114, 2000.
17. V. A. Juvekar and M.M. Sharma, Absorption of CO_2 in a suspension of lime, Chemical Engineering Science, vol. 28, 825-837, 1973.
18. Keith J. Laidler, Chemical Kinetics, 2nd edition, McGraw-Hill, Inc, New York, 1956.
19. O. Levenspiel, Chemical Reaction Engineering, 3rd Edition, John Wiley and Sons, New York. 1999.
20. H.F.W. Taylor, Cement Chemistry, Academic Press Inc., San Diego, CA, 128, 1990.
21. Charles M. Earnest, Modern Thermogravimetry, Analytical Chemistry, vol. 56, no. 13, 1471A-1486A, 1982.
22. W.M. Groenewoud and W. deJong, The thermogravimetry analyser – coupled – Fourier transform infrared/mass spectrometry technique, Thermochimica Acta, vol. 286, 341-354, 1996.
23. Peter R. Nelson, Marie Coffin and Karen A.F. Copeland, Introductory Statistics for Engineering Experimentation, Elsevier Science, USA, 2003.
24. Robert S. Boynton, Chemistry and Technology of Lime and Limestone, 2nd edition, John Wiley and Sons, 1980.
25. Edward J. Anthony, Lufei Jia, Yinghai Wu, CFBC ash hydration studies, Fuel, vol. 84, 1393-1397, 2005.
26. E.J. Anthony and L. Jia, Carbonation of FBC Ash using Sonic Energy, Journal of Solid Waste Technology and Management, vol. 30, no. 4, 212 -220, 2004.
27. E.J. Anthony, L. Jia, L. Cyr, B. Smith, and S. Burwell, The Enhancement of Hydration of Fluidized Bed Combustion Ash by Sonication, J. Environ. Sci. Tech., vol. 36, no. 20, 2002.
28. Edward J. Anthony, Agripina P. Iribarne, Julio V. Iribarne and L. Jia, Reuse of landfilled FBC residues, Fuel, vol. 76, no.7, 603-606, 1997.
29. D. Gora, E.J. Anthony, E.M. Bulewicz, L. Jia, Steam reactivation of 16 bed and fly ashes from industrial-scale coal-fired fluidized bed combustors, Fuel, vol. 85, 94-106, 2006.
30. Wesley W.M. Wendlandt, Thermal methods of analysis, Interscience Publishers, New York, 101-102, 1964.